NATIONAL ADVISORY COMMITTEE FOR AERONAUTICS

TECHNICAL NOTE 3878

THEORETICAL AND EXPERIMENTAL INVESTIGATION OF RANDOM GUST LOADS. PART I - AERODYNAMIC TRANSFER FUNCTION OF A SIMPLE WING CONFIGURATION IN INCOMPRESSIBLE FLOW

By Raimo J. Hakkinen and A. S. Richardson, Jr.

Massachusetts Institute of Technology

Washington

May 1957

NATIONAL ADVISORY COMMITTEE FOR AERONAUTICS

TECHNICAL NOTE 3878

THEORETICAL AND EXPERIMENTAL INVESTIGATION OF RANDOM GUST LOADS. PART I - AERODYNAMIC TRANSFER FUNCTION OF A SIMPLE WING CONFIGURATION IN INCOMPRESSIBLE FLOW

By Raimo J. Hakkinen and A. S. Richardson, Jr.

SUMMARY

Measurements of sinusoidally oscillating downwash and lift produced on a simple rigid airfoil have been made. Comparison with theory indicates agreement in order of magnitude and trend, although the scatter of results precludes their use for direct verification of Sears' gust function. Necessary improvements in experimental techniques are discussed.

Measurements of statistically stationary random downwash and corresponding lift on a simple rigid airfoil have been made and values of the transfer function between their power spectra determined. An approximate analysis has been carried out and the results are compared with the present experimental results as well as with those of another investigation. Reasonable agreement is shown at high reduced frequencies. A more extensive measurement program is recommended.

INTRODUCTION

Until recently, the emphasis in investigations of aircraft gust loads has been on the response to a single gust. Flight test programs, beginning with Doolittle's work in 1924 (ref. 1), have been carried out in order to determine a reasonable "maximum" gust velocity for airworthiness requirements (refs. 2 and 3). Theoretical considerations, following the fundamental papers of Rhode and Lundquist (ref. 4) and of Küssner (ref. 5), have dealt primarily with methods for computing the transient response of an aircraft to such a single gust.

In reality, however, atmospheric turbulence does not generally consist of single gusts but is a continuous random process. An airplane flying through disturbed air experiences a load history which is a randomly oscillating function of time. It is therefore apparent that an analysis of gust loads based on the concept of a random process instead

of that of a single gust would be much closer to the physical nature of the problem and could also be expected to yield more realistic and significant results. Unfortunately, the necessary mathematical techniques had been lacking until Wiener's generalized harmonic analysis (e.g., ref. 6) was applied to practical problems in engineering and research (ref. 7).

By treating the atmospheric turbulence as a statistically stationary process and by making use of the response of an aircraft to a purely sinusoidal disturbance, the generalized harmonic analysis provides relations between the power spectral densities of the fluctuations of the vertical velocity component and of the lift experienced by the airplane. In general, if these power spectra are denoted by Φ_V and Φ_L, respectively, and the sinusoidal transfer function of the aircraft, by $\Gamma(\omega)$, and if the effects of spanwise variation of the instantaneous downwash are neglected, one obtains

$$\Phi_{LL}(\omega) = \left(\frac{dC_L}{d\alpha}\frac{qbc}{U}\right)^2 \left|\Gamma(\omega)\right|^2 \Phi_{VV}(\omega)$$

A similar result was utilized by Clementson in 1950 (ref. 8) for deducing power spectra of atmospheric turbulence from the measurements of pitch response of aircraft in flight. At the same time, Liepmann computed the response of an airfoil to turbulent velocity fluctuations (refs. 9 and 10). Since these reports, several papers have been published about the gust-load problem (refs. 11 to 17) as well as about the "inverse" problem of atmospheric turbulence measurements (refs. 18 and 19).

The present research program at the Massachusetts Institute of Technology was motivated by the lack of experimental proof of the validity of the new method. Except for concurrent work (ref. 13), there were no investigations which could provide such a proof. In fact, even the two-dimensional sinusoidal response function, which was computed by Sears in 1941 (ref. 20), had never been satisfactorily verified experimentally. It was therefore decided to undertake the following two-phase program:

(1) To create a sinusoidal cross-velocity fluctuation in a low-speed wind tunnel and to measure its characteristics, as well as the characteristics of the lift fluctuation on an airfoil of simple geometric configuration exposed to the velocity fluctuations. From the measurements one can then obtain experimental values of the transfer function which are directly comparable with Sears' gust function.

(2) To create a random but statistically stationary velocity disturbance field in a low-speed wind tunnel and to measure the power spectra of fluctuations of velocity and of lift on a rigid airfoil. From the

measurements one can again obtain experimental values of the amplitude gain of the transfer function, and a comparison with theoretical results can be made.

During the course of the investigation, several problems which were secondary to the main objective turned out to be of importance. One of these is the effect of spanwise variation of the turbulent velocity fluctuation, which modifies the sinusoidal transfer function much more than was originally expected. Another problem to which considerable effort had to be devoted is that of the measurement of statistical quantities with sufficient accuracy.

This research was conducted under the sponsorship and with the financial assistance of the National Advisory Committee for Aeronautics.

SYMBOLS

A	area of force-sensitive wing section, sq in.
a_w'	hot-wire overheating ratio, $\frac{R_w - R_e}{R}$
$a(\omega,\omega_0)$	filter response curve
b	span of force-sensitive wing section, in.
Ci	cosine integral, $Ci(\xi) = -\int_{\xi}^{\infty} \frac{\cos \xi'}{\xi'} d\xi'$
C_L	lift coefficient
c	chord, in.
$F(\omega_0)$	filter factor, radians/sec
f	filter output, mv
g	span-effect correction factor
$H_0^{(2)}, H_1^{(2)}$	Hankel functions
h	lift influence function, $in.^{-2}$

$\bar{h}$ wing oscillation amplitude, in.

h_o strip-theory lift influence function, $in.^{-2}$

h_b total lift influence function, $in.^{-2}$

I hot-wire current, ma

I_o hot-wire calibration constant, ma

J_o, J_1 Bessel functions of first kind

K_o, K_1 modified Bessel functions of second kind

k reduced frequency

k_1 streamwise wave number, radians/in.

k_2 spanwise wave number, radians/in.

L lift, lb

l streamwise distance, in.

Q filter-band-width parameter in $\left|a(\omega,\omega_o)\right|^2 = \dfrac{1}{1 + 4Q^2\left(\dfrac{\omega - \omega_o}{\omega_o}\right)^2}$

q dynamic pressure, psi

R_e hot-wire cold resistance, ohms

R_w hot-wire working resistance, ohms

r hot-wire output tapping ratio

S Sears' gust function

Si sine integral, $Si(\xi) = \int_0^{\xi} \dfrac{\sin \xi'}{\xi'} d\xi'$

s thermocouple output, mv

T integration time, sec

T_c thermocouple time constant, sec

t	time, sec
U	stream velocity, mph and in./sec
u	streamwise velocity fluctuation, in./sec
v	crosswise velocity fluctuation, in./sec
x	streamwise coordinate, in.
y	spanwise coordinate, in.
α	angle of attack, radians
β,ϵ	dimensionless variable in g
Γ	transfer function in one variable
$\tilde{\Gamma}$	transfer function in two wave numbers
γ	dimensionless thermocouple time constant
η	spanwise distance variable
Λ	turbulence scale, in.
ν	hot-wire output voltage, mv
ξ	streamwise distance variable, in.
ρ	dimensionless integration time
σ	root-mean-square error
τ	time variable, sec
Φ_{LL}	lift power spectrum
$\Phi_{s_1 s_1}$	power spectral density of input
Φ_{vv}	power spectral density of v in one variable, $(\text{in./sec})^2(\text{radians/in.})^{-1}$
$\tilde{\Phi}_{vv}$	power spectral density of v in two wave numbers, $(\text{in./sec})^2(\text{radians/in.})^{-2}$
φ_{LL}	lift correlation function
φ_{ss}	normalized correlation function of $s(t)$

Φ_{vv} correlation function of v in one variable, $(in./sec)^2$

$\tilde{\Phi}_{vv}$ correlation function of v in two variables, $(in./sec)^2$

ψ hot-wire angle, radians

$\bar{\Omega}$ reduced circulation amplitude, in./sec

ω circular frequency, radians/sec

GENERAL EXPERIMENTAL EQUIPMENT

Wind Tunnel

All measurements were performed in the 5- by $7\frac{1}{2}$-foot low-speed wind tunnel of the M.I.T. Aeroelastic and Structures Research Laboratory. This tunnel has a maximum speed of approximately 100 mph. However, in order to avoid excessive overheating of the tunnel during long runs most of the present measurements were made at a speed of 50 mph.

Since this wind tunnel was originally built for flutter investigations, no special care was taken in its design to obtain a low turbulence level. As shown in figure 1, both the contraction ratio and the distance from the turning vanes to the test section are relatively small. A turbulence level of the order of one-quarter of 1 percent root mean square of the free-stream velocity was measured at a speed of 50 mph with an uncompensated 0.00015-inch tungsten hot-wire, which has a frequency-response cutoff around 200 cps.

The tunnel velocity was generally measured by means of a pitot-static probe and an inclined-tube alcohol manometer. In hot-wire calibrations, very low velocities (of the order of 3 fps) were needed and the vortex-frequency technique described in reference 21 was successfully used. In the overlapping region of the ranges of the two velocity measuring devices an agreement within about 2 percent was generally obtained.

Hot-wire surveys of the flow indicated satisfactorily uniform conditions in the region where measurement apparatus was located.

Measurement of Velocity Fluctuations

As will be described in the succeeding sections, additional velocity fluctuations were introduced into the mean flow by mechanical devices. The component of these fluctuations normal to the test airfoil was measured by means of a directionally sensitive hot-wire probe. This probe

consisted of two approximately 0.05-inch-long and 0.00015-inch-diameter tungsten wires in the form of an X. The probe was mounted on a vertical stand and could be both moved vertically and turned in the horizontal plane by remote control. The horizontal position of the stand could be adjusted between runs. A special rigid-base structure attached directly to the building walls was brought in through holes in the tunnel floor and ceiling in order to minimize vibrations of the probe. Figure 2 shows the probe in position.

Facilities for manufacture and repair of the hot-wire probes were set up at the laboratory. After some initial difficulties, no trouble beyond occasional breakage and dirt collection was experienced.

Electrical Circuit

It is difficult to produce two exactly identical wires for a double-wire probe. Consequently, in order to obtain pure lateral-velocity response, the heating currents in the two wires must be individually adjustable. Therefore, a circuit consisting of two separate Wheatstone bridges was built (fig. 3). Currents were measured by reading the voltage drop across a precision resistor on a Rubicon potentiometer. Bridge balance was observed on a Weston sensitive galvanometer.

Calibration of Hot-Wire Probes

The conditions for operating a double oblique-wire probe with pure cross-velocity sensitivity are derived in appendix A. First, an individual calibration of each wire is needed for determination of the calibration constants, from which the current and voltage divider settings can be calculated. Such calibrations were made normally at four velocities and two values of the overheating ratio. Calibration of the cross-velocity sensitivity was obtained by turning the probe in a horizontal plane through known angles. Independence of fluctuations in the streamwise direction was finally ascertained by observing the probe response while tunnel speed was varied within ±10 percent about the operating condition. Typical single-wire and cross-velocity calibrations are presented in figures 4 and 5, respectively.

Satisfactory linearity and repeatability were generally obtained in the calibrations. Occasionally it was found, however, that after a long time of operation the calibration changed slightly because of collection of dirt on the wires. After cleaning the probe, the original calibration was usually obtained, in some cases with remarkable accuracy. The wires were cleaned with ether every day before runs were started, and it is not believed that serious errors could have been introduced into the measurements by the dirt deposits.

Since the frequency range of interest in the present investigation extended only up to about 150 cps, no compensating circuits were used for the 0.00015-inch tungsten wires.

Measurement of Lift Fluctuations

Since it was desired to obtain measurements of lift produced by turbulence on a simple airfoil configuration, a constant-cross-section wing spanning the 5-foot tunnel height was installed on the same rigid supporting structure as the hot-wire stand. The wing chord was chosen to be 1 foot in order to provide a reasonably high Reynolds number (500,000 at 50 mph tunnel speed). The profile is NACA 0010.

The main structure of the wing consisted of two full-span 1- by $\frac{5}{16}$-inch steel beams and two $\frac{1}{8}$- by $2\frac{3}{4}$-inch steel flanges, bolted together. Profile shape was obtained by attaching balsa blocks to the steel parts. In the center of the wing, a 4-inch-span section was cut off, except for the two main steel beams, and replaced by a load-sensitive element mounted on strain-gage pickups. Figure 6 shows details of the wing.

The load-sensitive section consisted of two hollowed balsa blocks joined together by thin curved magnesium plates. One of the plates was supported by three strain-gage load cells in such a manner that the section "floated" about the throughgoing steel structure. Thus, a lift load on the section was indicated as the sum of the signals from the three pickups. The load cells were manufactured by the Dynamic Instrument Co. Each one consisted of unbonded strain gages, arranged as a four-active-arm Wheatstone bridge, supporting a steel pin which protruded through the end of the cylindrical-shape pickup. Dimensions of the pickup were small enough to permit complete internal mounting within the 1.2-inch-thick airfoil (see fig. 6). Connection to the magnesium plate was made by means of a brass bushing and soft soldering. Current to each load pickup was supplied by a separate dry cell, and the outputs were connected in series. Figure 7 shows the circuit diagram and figure 8, a typical calibration of one pickup. Before each series of runs, a calibration of the complete system was made and its independence of the point of application of the load was checked.

The principal consideration in the design of the lift sensing system was to obtain a mechanism rigid enough to avoid excessive displacements and resonance peaks in the important frequency range (below 200 cps). Both of these purposes were satisfactorily accomplished; the displacements were of the order of 0.001 inch or less, and a natural frequency of 330 cps was obtained. The dynamic response was tested by means of an electromagnetic shaker. The floating wing section and the pickups were mounted on an exact duplicate of the local wing-span structure (shown in fig. 6) and shaken at constant acceleration throughout the desired frequency range.

In the first tests, a strong resonance peak was obtained at around 200 cps. It disappeared completely, however, after stiffening the structure of the floating section by cementing strips of magnesium sheet to the sides of the rear balsa block.

A serious problem was presented by the vibration of the entire wing structure due to the turbulence acting on it. The wing had a natural bending frequency of only approximately 25 cps and considerable vibration was therefore present at the load cell mountings. Instead of trying to stiffen the wing structure by guy wires or otherwise, it was decided to install a separate pickup inside the floating section so that it would respond to only the structural vibrations. By suitable adjustments of the feeding voltage and of a dummy mass attached to the pickup, the dynamic responses of the two systems could be made nearly identical. Thus, if the signal of the dummy system was reversed and connected in series with the main signal, the structural vibrations would cancel out and a signal indicating the pure aerodynamic force could be obtained. The electromagnetic shaker was again used for verification of the cancellation performance. The measured dynamic response curves, referred to the uncompensated value at zero frequency, are presented in figure 9.

It should be noted that, while the cancellation is very effective at low frequencies, considerable errors appear at certain frequencies and especially around the resonance. Since, however, there is an appreciable reduction in the support vibration response throughout the frequency range under investigation (even in the worst case at 150 cps the cancellation is about 75 percent), it was not considered necessary to improve the performance by closer matching of damping characteristics or other methods.

As far as support vibrations in pitch and roll are concerned, their effects can theoretically be shown to cancel out if the center of gravity of the floating section is placed in the exact geometric center of the triangle formed by the three pickups and if the dummy pickup is located at that same point. The first condition was satisfied exactly by use of small lead weights in the front balsa block. In the second one, a small error was necessary because of space requirements. In any case, in view of the relatively high torsional rigidity of the wing, the pitch and roll vibrations are believed to be of secondary importance.

The static aerodynamic response of the lift sensing system was obtained experimentally by turning the wing about a vertical axis to known values of angle of attack. The resulting lift-curve slope was 0.08 per degree with excellent linearity through the $\pm 7^{\circ}$ range covered in the measurement.

Auxiliary Equipment

A two-channel amplifier was designed and built for use with both hot-wire and lift signals. The amplifier operates on the push-pull principle and has a one-side maximum gain of 2,400, with a noise level of

approximately 100 microvolt referred to the input. The noise was, however, found to consist largely of 120-cps pickup and could be avoided in the spectrum measurements. Frequency response of the amplifier was flat from 0.5 cps to several kilocycles. Circuit diagram, amplitude calibration, and frequency response are shown in figures 10, 11, and 12, respectively.

By means of a switching circuit, amplifier inputs could be selected from either external sources or from the bridge circuit, such as the hot-wire signals, their difference and sum, and so forth. The amplifier output was available as push-pull or low-impedance cathode follower signals or could be fed into a heater-thermocouple unit through a driver stage (fig. 13).

The heater-thermocouple unit produces a smoothed square of the input signal. Calibrations for steady direct current or sinusoidal signals are given in figure 14. For random signals the output fluctuates, making visual reading of the mean-square value difficult. To minimize this fluctuation, units with a time constant of 5 seconds were obtained from the Cambridge Instrument Co. in England. Nevertheless, it turned out to be necessary to average the thermocouple output more accurately by integrating it over a long period of time (see section on turbulence measurements) by means of a Miller type integrator. The integrator consisted of a Reeves direct-current amplifier and a 1-microfarad condenser connected between input and output; it has the calibration shown in figure 15.

RESPONSE OF RIGID AIRFOIL TO SINUSOIDAL GUSTS

Experimental Techniques

The sinusoidal velocity fluctuations were generated by a 1-foot-chord, 5-foot-span wing which was rigidly mounted on a horizontally oscillating steel rod at the upstream end of the test section (see fig. 16). The maximum amplitude of the translatory oscillation was approximately 2 inches and the practical frequency range extended up to 10 cps, although at the higher frequencies the amplitude had to be considerably decreased owing to considerations of wing strength and rigidity of the oscillator mechanism. The wing had an NACA 0012 airfoil and a magnesium-skin balsa structure.

The velocity fluctuations and lift produced on the stationary wing were measured by the hot-wire and strain-gage equipment described in the preceding section. The frequency of the moving-wing oscillation was measured by means of a microswitch and a Hewlett-Packard electronic counter.

The root-mean-square sinusoidal gust velocity was found to be less than one-half of 1 percent of the free-stream velocity. Although both

the velocity and lift signals were well within the useful range of their respective sensing units, they could not be satisfactorily distinguished from the effects of the relatively high free-stream turbulence level of the wind tunnel. It was therefore decided to filter the signals electrically by means of a General Radio 762-B vibration analyzer. This instrument has a narrow-band-pass characteristic, with a value of the Q-parameter of about 80.

Use of the narrow-band filter greatly reduced the effects of background turbulence. However, a new difficulty appeared because of a drift in the oscillator frequency of the order of ± 0.5 percent of its mean value. With the narrow-band-pass filter, this drift caused fluctuations in the measured signal of about ± 30 percent. It was estimated that in order to decrease this figure to a satisfactory level a frequency drift of only ± 0.1 percent would be permissible. The obvious remedies would be either to obtain a better frequency control for the oscillator or to use a filter with a wider flattop characteristic curve. Both of these measures would, however, have required design and construction of precision machinery or accurate electronic circuits and involved considerable effort and expense beyond the resources of the present program.

It was originally planned to obtain measurements of the phase angle as well as of the amplitude gain of the Sears' function. Unfortunately, the phase shift in the band-pass filter unit turned out to depend strongly on the signal amplitude and accuracy of tuning, thus making the phase measurement impractical. After the experiences described above, it was concluded that the only way to obtain satisfactory measurements of the Sear's function would be to perform the experiments in a tunnel with a low background-turbulence level and with an oscillator mechanism which would be capable of producing large downwash amplitudes. It is believed that significant improvements can be made in both of these items in the present wind tunnel, but only after considerable effort and expense.

A question was raised regarding the possibility that even with absolutely steady oscillator frequency the sinusoidal downwash pattern downstream may have a tendency to "contract" and "expand" in response to low-frequency disturbances in the streamwise velocity, thus producing hot-wire and lift signals which would exhibit a frequency drift. The present instrumentation could not provide conclusive results about this suspected phenomenon; it is, however, believed to be worthy of further investigation.

In spite of these difficulties, it was decided to make such measurements as were possible in order to gain experience for further work. The measurements for downwash and lift amplitudes were made in separate runs with the hot-wire mount and the rigid wing in approximately the same position. Actually, because of structural reasons, the hot-wire was located about 1/2 chord upstream of the wing leading edge; however, since phase measurements were not attempted, the resulting error is negligible.

Measurement of Sinusoidal Velocity Fluctuations

After filtering, the hot-wire signal was amplified and its mean square was determined by means of the heater-thermocouple unit. Since considerable fluctuation was observed in the thermocouple output, integration over several minutes was necessary. The system diagram is presented in figure 17.

By shutting off the oscillator system, it was possible to determine the mean-square value of the combination of remaining background turbulence and amplifier noise. Subtraction of this value from the mean square of the total signal should then provide the mean square of the pure sinusoid. This correction cannot, however, account for any effects of the frequency drift. Figure 18 shows sample recordings of the hot-wire signal taken by means of a Brush oscillograph.

For calibration purposes, a known sinusoidal signal was injected into the filter input. Frequency of the calibration signal was determined by comparing it against the oscillating-wing frequency on a Hewlett-Packard counter. Considerable scatter is shown in the results (fig. 19).

Measurement of Sinusoidal Lift Fluctuations

A somewhat different technique was used for analysis of the lift signals. For reasons which are not completely understood, a considerably lower noise level was observed in the lift signal than in the hot-wire output. In part this is believed to be caused by some high-frequency noise leaking through the filter, as was observed to happen to some extent in the hot-wire measurements. Because of the aerodynamic response characteristics of the wing, much less such noise is present in the strain-gage signal.

The amplitude of the lift signal could now be obtained as an average of several visual readings on an oscilloscope at short intervals (fig. 20). The calibration signal, its frequency determined as in the case of the hot-wire measurements, was also observed on the oscilloscope.

The results (fig. 21) show somewhat less scatter than the downwash measurements.

Theoretical Considerations

According to Ashley (ref. 22), the downwash in the plane of the wake behind a two-dimensional wing in sinusoidal oscillation can be expressed as follows, provided that the point of observation is sufficiently far from the wing (distance l from midchord):

$$v(l,t) = -\frac{\bar{\Omega}}{2\pi} e^{i\omega t}\left(e^{-ik}\left[1 - \sqrt{\frac{(2l/c) - 1}{(2l/c) + 1}}\right] + ke^{-\frac{2ikl}{c}}\left\{\frac{\pi}{2} + \mathrm{Si}\left[k\left(\frac{2l}{c} - 1\right)\right] - i\,\mathrm{Ci}\left[k\left(\frac{2l}{c} - 1\right)\right]\right\}\right)$$

where Si and Ci are the sine and cosine integrals, respectively, and the reduced circulation amplitude is

$$\bar{\Omega} = \frac{4\int_{-1}^{1}\sqrt{\frac{1+\xi'}{1-\xi'}}\,\bar{v}_o(\xi')d\xi'}{\pi ik\left[H_1^{(2)}(k) + iH_o^{(2)}(k)\right]}$$

and where $\bar{v}_o(\xi')$ is the local amplitude of the wing oscillation velocity as a function of chordwise position $\xi' = x/\frac{c}{2}$. In the present case of translatory motion with amplitude $\bar{h}$,

$$\bar{v}_o(\xi') = -i\omega\bar{h}$$

and

$$\bar{\Omega} = \frac{4U\left(\bar{h}/\frac{c}{2}\right)}{H_1^{(2)}(k) + iH_o^{(2)}(k)}$$

By substitution, the complex downwash amplitude becomes

$$\bar{v}(l) = -\frac{2}{\pi}U\left(\frac{\bar{h}}{c/2}\right)\frac{\exp(-ik)}{H_1^{(2)}(k) + iH_o^{(2)}(k)}\left(1 - \sqrt{\frac{\frac{2l}{c} - 1}{\frac{2l}{c} + 1}} + ke^{-ik\left(\frac{2l}{c} - 1\right)}\left\{\frac{\pi}{2} + \mathrm{Si}\left[k\left(\frac{2l}{c} - 1\right)\right] - i\,\mathrm{Ci}\left[k\left(\frac{2l}{c} - 1\right)\right]\right\}\right)$$

A plot of the absolute amplitude of the downwash angle $\left(\frac{\bar{v}}{\bar{U}}\right)\Big/\left(\frac{2\bar{h}}{c}\right)$ is given in figure 19 for the present case of $2l/c \pm 13$. Since the measured lift-curve slope of the wing is only 4.58 per radian instead of the theoretical 2π per radian, a corresponding correction has been made to the plotted curve.

The sinusoidal lift produced by this downwash on another two-dimensional wing of the same chord has an amplitude (assuming that the downwash over the wing is constant and equal to the calculated value at midchord) of

$$\bar{L} = \left[\frac{\bar{v}(l)}{U}\right](2\pi)\left[S(k)\right](qA)$$

where $S(k)$ is the Sears' gust function.

The absolute dimensionless amplitude $\left|\frac{\bar{L}}{\frac{2\bar{h}}{c}qA}\right| = \left|\frac{\bar{C}_L}{2\bar{h}/c}\right|$ is plotted in figure 21. Since the measured steady-state lift-curve slope of the lift-sensing wing is $dC_L/d\alpha = 4.58$ per radian, this value was again substituted for the theoretical 2π per radian.

Discussion

Because of the scatter of the measurements, it was not possible to compare the results directly with the results of Sears' gust function. The measured lift, however, agrees reasonably well with the theoretical prediction.

The equipment developed for measuring downwash and lift was found to be satisfactory. However, a much lower ratio of background turbulence to sinusoidal downwash in the wind tunnel and a better frequency control of the oscillator are required for successful completion of conclusive measurements.

RESPONSE OF A RIGID AIRFOIL TO RANDOM GUSTS

Experimental Technique

For measuring the random downwash and the associated lift response of a rigid airfoil, the equipment described in the preceding sections was again

used. Both the hot-wire and the lift-sensing wing were placed in the center of the test section approximately 2 feet apart in order to permit simultaneous measurements of lift and downwash. This arrangement eliminates errors due to differences in operating conditions in separate runs. It is not believed that interference effects large enough to offset this gain could have been introduced into the turbulence field.

The downwash fluctuations were generated by a coarse grid installed approximately 10 feet upstream of the measuring units (fig. 22). The mesh size of the grid was 6 inches, which was considered to be a maximum for maintaining a reasonably homogeneous turbulence field in the test area. The grid members were 1 inch wide with a square cross section.

Unfortunately, the turbulence scale obtainable with this grid is, at most, of the order of the mesh size, that is, less than a half-chord of the wing. In atmospheric turbulence, scales much larger than the chord length of an average airplane are generally encountered (ref. 8). Naturally, a closer matching could be obtained by decreasing the model size; this, however, would result in very low Reynolds numbers, with associated adverse aerodynamic effects, as well as in instrumentation difficulties.

A hot-wire survey of the turbulence level in the test area showed homogeneity of the root-mean-square fluctuation to tunnel velocity ratio within approximately 5 percent. The average value of this ratio was approximately 0.03. A background-turbulence level of about one-fourth of 1 percent root mean square was observed in the empty tunnel. The turbulent fluctuations are therefore actually generated by two separate sources, although the contribution of the grid is dominating. Since the power spectral density of the total turbulent downwash is measured, the dual origin does not present serious complications.

Recording and Analysis of Data

In order to avoid excessively long running times with associated changes in tunnel operating conditions, both the hot-wire and lift signals were recorded simultaneously on magnetic tape by means of an Ampex 306 two-channel recorder. The recording time was generally several minutes and was determined on the basis of accuracy considerations which will be discussed subsequently. The system diagram is presented in figure 23.

The power spectra were determined by playing the recorded signal into the thermocouple squaring unit through a narrow-band-pass filter set at different frequencies. A General Radio 732-B vibration analyzer was used as the filter. This instrument has a Wien bridge circuit with a band-pass parameter $Q = 80$ and a range from 2.5 to 750 cps.

Some difficulty was experienced in the calibration of the vibration analyzer. If the frequency-response curve of the filter at central frequency ω_0 is $a(\omega,\omega_0)$, the output signal s_2 is related to the power spectrum of the input s_1 as follows:

$$\overline{s_2^2} = \int_{-\infty}^{\infty} \left|a(\omega,\omega_0)\right|^2 \Phi_{s_1 s_1}(\omega)\,d\omega$$

If $\Phi_{s_1 s_1}$ is constant or, in case of a symmetrical (with respect to ω_0) $\left|a(\omega,\omega_0)\right|$ curve, linear over the effective filter range, one can simplify

$$\overline{s_2^2} = \Phi_{s_1 s_1}(\omega_0) \int_{-\infty}^{\infty} \left|a(\omega,\omega_0)\right|^2 d\omega = \Phi_{s_1 s_1}(\omega_0) F(\omega_0)$$

Thus, the filter response factor $F(\omega_0)$ is needed for quantitative evaluation of power spectrum by the method described above. A careful measurement of the response curve $\left|a(\omega,\omega_0)\right|$ was made for selected frequencies by actually determining the attenuation of a steady sinusoid in the filter range. Then $F(\omega_0)$ was computed by manual integration of $\left|a(\omega,\omega_0)\right|^2$. Unfortunately, it was found later that the calibration of the vibration analyzer was very sensitive to any changes in battery voltages and component characteristics. Since, for instance, batteries and tubes had to be replaced during the course of the measurements and a complete recalibration every time would have been impractical, it was decided not to attempt accurate absolute measurements of power spectra.

The main purpose of the experiments, to obtain values of the transfer function connecting the input and output power spectra, could be accomplished without knowledge of $F(\omega_0)$. Since the hot-wire and strain-gage outputs were recorded on magnetic tape, it was possible to run both signals through the filter successively, so that changes in the filter between the runs were very unlikely. Thus, even though the measured mean-square values could not be absolutely evaluated to give the two power spectral densities, the unknown proportionality factors were identical and canceled out in computation of the transfer function. The experimental results presented in figure 24 were determined in this manner. The physical frequency range of the measurements is from 3 to 150 cps. An additional dynamic-response correction corresponding to figure 9 was applied to the lift measurements at high frequencies.

Accuracy of Measurements

The errors in the present measurements can be divided into the following two categories:

(1) Measurement errors, arising from changes in the equipment response, inaccuracies in calibration, reading errors, and so forth. It is difficult to estimate the total probable error of a system as complicated as the one used here. The accuracy of voltmeters and other instruments used in calibrating individual parts of the system is generally within ±1 to ±3 percent. Repeatability of the hot-wire calibrations is of the same order, and inevitable changes occur in the electronic circuits because of tube aging, line voltage fluctuations, and so forth. Therefore, a total error of several percent has to be considered probable.

(2) Statistical errors, arising from the fact that the power spectral densities are measured as finite time averages. Since the power spectral density can be considered an infinite time average of the filtered and squared signal, a measurement over a finite time has to suffer in accuracy. Fortunately, it is possible to estimate this error on the basis of results presented by Rice (ref. 7). Such an analysis applicable to the present measurements is presented in appendix B.

The calculated root-mean-square error curves in figure 25 were used in choosing averaging times at each selected frequency. In general, a root-mean-square error of 3 percent was planned for in the power-spectrum measurements. The experimental value of the transfer function, computed as the ratio of two such spectrum measurements, could then be expected to have a statistical root-mean-square error of the order of 5 percent. One has to realize, however, that these numbers refer to the root-mean-square error of an infinite ensemble of measurements performed under identical conditions. All that can be said regarding an individual measurement is to state its probability of being within specified limits of error. For instance, if the probability density distribution of the transfer function is assumed to be Gaussian (approximate analysis indicates that this may not be an unreasonable assumption), a 5-percent root-mean-square error implies that a single measurement would have an approximately 90-percent probability of being within ±10 percent of the correct value.

A series of individual measurements at different frequencies would show scatter of the order of the root-mean-square error. In the present case, it is not possible to say definitely whether the few points at low frequencies reflect an unduly large scatter or an anomalous behavior of the transfer function as compared with the theoretical estimate. At higher frequencies, where the computed averaging times were also generally exceeded for practical reasons, the scatter is of acceptable magnitude.

The best way to increase the reliability of the present results would be to obtain a large number of power-spectrum measurements at each selected frequency. The average of such measurements would be essentially equivalent to a result obtained by using a longer, otherwise impractical, averaging time. The statistical accuracy would be correspondingly improved and some measurement errors of random nature would also be minimized.

Theoretical Considerations

The measured characteristics of the turbulent downwash fluctuations and the corresponding lift on an airfoil are the power spectral densities Φ_{vv} and Φ_{LL} in terms of the reduced frequency $k = \omega c/2U$ or the streamwise wave number $k_1 = \omega/U$. The transfer function Γ is then obtained from these two spectral densities as follows:

$$\left|\Gamma(k_1)\right|^2 = \frac{\Phi_{LL}(k_1)}{\Phi_{vv}(k_1)}\left(\frac{U}{\frac{dC_L}{d\alpha}_{qbc}}\right)^2$$

If the velocity disturbance field were variable in the stream direction only, so that the instantaneous angle of attack were constant along the span, the transfer function $\Gamma(k_1)$ would be identical with the transfer function for a wing passing through a sinusoidal gust field. For a wing of constant cross section and infinite span this is the Sears' gust function (ref. 20):

$$S(k) = \frac{J_0(k)K_1(ik) + iJ_1(k)K_0(ik)}{K_1(ik) + K_0(ik)}$$

Unfortunately, in reality random velocity disturbances in the atmosphere as well as in a wind tunnel possess statistical characteristics which are (in most cases) very much the same in any direction the turbulence field may be traversed. Consequently, in trying to obtain a realistic estimate of the transfer function, one has to account for the spanwise variation of the instantaneous angle of attack. This brings in a new variable, the spanwise wave number k_2. An approximate two-wave-number analysis will now be carried out for the geometrical configuration used in the present experiments. The analysis follows essentially the line of thought presented by Liepmann (ref. 15). It should be emphasized that the general procedure is by no means restricted to the simple wing geometry and turbulence spectra considered herein.

Using the coordinate systems defined in figure 26 and assuming the validity of Taylor's hypothesis for the motion of the wing through the turbulence field $v(x,y)$, one can write the lift dL on a chordwise strip of width dy at y as

$$dL(x,y) = \frac{dC_L}{d\alpha}\frac{qc}{U}\,dy \iint_{-\infty}^{\infty} h\left(\xi, |\eta - y|\right) v(x - \xi,\eta)\,d\xi\,d\eta$$

where $h\left(\xi, |\eta - y|\right)$ is the influence function for lift per unit span at y produced by a unit downwash impulse at position (ξ,η) with respect to the wing. The total lift as a function of the position of the wing in the x-direction is then

$$L(x) = \left(\frac{dC_L}{d\alpha}\frac{qc}{U}\right) \int_{-b/2}^{b/2} dy \iint_{-\infty}^{\infty} h\left(\xi, |\eta - y|\right) v(x - \xi,\eta)\,d\xi\,d\eta$$

At this point it is convenient to introduce an integrated influence function

$$h_b(\xi,\eta) = \frac{1}{b}\int_{-b/2}^{b/2} h\left(\xi, |\eta - y|\right) dy$$

which represents the lift on the whole lift-sensitive section of span b due to a unit impulse downwash at (ξ,η) (see fig. 26). After substitution one obtains

$$L(x) = \frac{dC_L}{d\alpha}\frac{qcb}{U} \iint_{-\infty}^{\infty} h_b(\xi,\eta)\, v(x - \xi,\eta)\,d\xi\,d\eta$$

To bring in the power spectral density, one forms the correlation of $L(x)$, which is taken as an ensemble average over $L(x)L(x + \Delta x)$:

$$\overline{L(x)L(x + \Delta x)} = \left(\frac{dC_L}{d\alpha}\frac{qbc}{U}\right)^2 \iiint_{-\infty}^{\infty} h_b\left(\xi_1,\eta_1\right) h_b\left(\xi_2,\eta_2\right) \overline{v\left(x - \xi_1,\eta_1\right) v\left(x + \Delta x - \xi_2,\eta_2\right)}\,d\xi_1\,d\xi_2\,d\eta_1\,d\eta_2$$

If the turbulence field is homogeneous in the xy-plane, the ensemble average over the velocity product is independent of x and can be replaced by the two-dimensional autocorrelation $\tilde{\varphi}_{vv}\left[\Delta x + (\xi_1 - \xi_2), (\eta_1 - \eta_2)\right]$. Similarly, the lift correlation can be expressed independently of x, giving

$$\varphi_{LL}(\Delta x) = \left(\frac{dC_L}{d\alpha}\frac{qbc}{U}\right)^2 \int_{-\infty}^{\infty}\int_{-\infty}^{\infty}\int_{-\infty}^{\infty}\int_{-\infty}^{\infty} h_b(\xi_1,\eta_1)h_b(\xi_2,\eta_2)\tilde{\varphi}_v\left[\Delta x + (\xi_1 - \xi_2), (\eta_1 - \eta_2)\right] d\xi_1\, d\xi_2\, d\eta_1\, d\eta_2$$

Now, $\tilde{\varphi}_{vv}$ can be written in terms of its Fourier transform, the power spectrum $\Phi_{vv}(k_1,k_2)$, as

$$\tilde{\varphi}_{vv}\left[\Delta x + (\xi_1 - \xi_2), (\eta_1 - \eta_2)\right] = \int_{-\infty}^{\infty}\int \tilde{\Phi}_{vv}(k_1,k_2) e^{i\left[k_1(\Delta x+\xi_1-\xi_2)+k_2(\eta_1-\eta_2)\right]} dk_1\, dk_2$$

By substitution and interchanging the order of integration

$$\varphi_{LL}(\Delta x) = \left(\frac{dC_L}{d\alpha}\frac{qbc}{U}\right)^2 \int_{-\infty}^{\infty} e^{ik_1\Delta x}\left\{\int_{-\infty}^{\infty} \tilde{\Phi}_{vv}(k_1,k_2)\left[\int_{-\infty}^{\infty}\int h_b(\xi_1,\eta_1)\ \exp\, i(k_1\xi_1 + k_2\eta_1)\, d\xi_1\, d\eta_1 \int_{-\infty}^{\infty}\int h_b(\xi_2,\eta_2)\ \exp\, -i(k_1\xi_2 + k_2\eta_2)\, d\xi_2\, d\eta_2\right] dk_2\right\} dk_1$$

If one now defines a two-wave-number transfer function

$$\tilde{\Gamma}(k_1,k_2) = \int_{-\infty}^{\infty}\int h_b(\xi,\eta) e^{i(k_1\xi+k_2\eta)} d\xi\, d\eta$$

the lift correlation can be written

$$\varphi_{LL}(\Delta x) = \left(\frac{dC_L}{d\alpha}\frac{qbc}{U}\right)^2 \int_{-\infty}^{\infty} e^{ik_1\Delta x}\left[\int_{-\infty}^{\infty} \tilde{\Phi}_{vv}(k_1,k_2)\left|\tilde{\Gamma}(k_1,k_2)\right|^2 dk_2\right] dk_1$$

From the uniqueness of the Fourier transform it follows then that the lift power spectrum must be

$$\Phi_{LL}(k_1) = \left(\frac{dC_L}{d\alpha}\frac{qbc}{U}\right)^2 \int_{-\infty}^{\infty} \left|\tilde{\Gamma}(k_1,k_2)\right|^2 \tilde{\Phi}_{vv}(k_1,k_2)dk_2$$

Hence, instead of Sears' function, one obtains a two-wave-number transfer function $\tilde{\Gamma}(k_1,k_2)$ and consequently also has to deal with a two-wave-number turbulence spectrum $\tilde{\Phi}_{vv}(k_1,k_2)$.

In trying to obtain an analytical expression the result of which could be compared with the experimental result, it is seen from the above that only $\Phi_{LL}(k_1)$ is measured directly. The measured turbulence spectrum $\Phi_{vv}(k_1)$ is related to $\tilde{\Phi}_{vv}(k_1,k_2)$ through integration as follows:

$$\Phi_{vv}(k_1) = \int_{-\infty}^{\infty} \tilde{\Phi}_{vv}(k_1,k_2)dk_2$$

Furthermore, there are no accurate aerodynamic theories for a calculation of $\tilde{\Gamma}(k_1,k_2)$. Consequently, one is forced to make the following simplifying assumptions in order to establish a comparison with the experimental results:

(1) It is assumed that the lift influence function follows the aerodynamic strip theory; that is, the lift at any spanwise position y on the wing depends only on turbulence at $\eta = y$. This leads to

$$h(\xi,|\eta - y|) = h_o(\xi)\delta(\eta - y)$$

$$h_b = \frac{1}{b} h_o(\xi) \qquad \left(|\eta| \leq \frac{b}{2}\right)$$

$$h_b = 0 \qquad \left(|\eta| > \frac{b}{2}\right)$$

The strip-theory assumption is certainly not correct, because it eliminates all effects due to the semi-infinite wing extensions. The resulting approximate formulas are therefore identical with those derived with the

same assumptions for a finite-span rectangular wing. Too high lift values can be expected, especially at a low aspect ratio. However, it is probable that in reality the "tails" of the influence function (fig. 26) die out rather rapidly, so that the error will decrease with increasing span. In any case, it is believed that no fundamental properties of the result would be lost because of application of strip theory.

(2) It is further assumed that the lift response of each strip is characterized by the Sears' function. Thus, $h_o(\xi)$ will be the Fourier transform of Sears' function, and one can write

$$\int_{-\infty}^{\infty} h_o(\xi) e^{ik_1\xi} d\xi = S\left(\frac{ck_1}{2}\right) = S(k)$$

By substitution, the two-wave-number transfer function then becomes

$$\tilde{\Gamma}\left(k_1,k_2\right) = \frac{1}{b}\int_{-b/2}^{b/2} e^{ik_2\eta} d\eta \left[\int_{-\infty}^{\infty} h_o(\xi) e^{ik_1\xi} d\xi\right]$$

$$\tilde{\Gamma}\left(k_1,k_2\right) = \frac{\sin\frac{bk_2}{2}}{bk_2/2} S\left(\frac{ck_1}{2}\right)$$

The lift power spectrum can now be written

$$\Phi_{LL}\left(k_1\right) = \left(\frac{dC_L}{d\alpha}\frac{qbc}{U}\right)^2 \left|S\left(\frac{ck_1}{2}\right)\right|^2 \int_{-\infty}^{\infty} \frac{\sin^2\frac{bk_2}{2}}{\left(\frac{bk_2}{2}\right)^2} \tilde{\Phi}_{vv}\left(k_1,k_2\right) dk_2$$

(3) In order to bring in the measured one-wave-number turbulence spectrum $\Phi_{vv}\left(k_1\right)$, the following span-correction factor is defined:

$$g\left(b,k_1\right) = \frac{\int_{-\infty}^{\infty} \frac{\sin^2\frac{bk_2}{2}}{\left(\frac{bk_2}{2}\right)^2} \tilde{\Phi}_{vv}\left(k_1,k_2\right) dk_2}{\int_{-\infty}^{\infty} \tilde{\Phi}_{vv}\left(k_1,k_2\right) dk_2}$$

The lift power spectrum becomes then

$$\Phi_{LL}(k_1) = \left(\frac{dC_L}{d\alpha}\frac{qbc}{U}\right)^2 \left|S\left(\frac{ck_1}{2}\right)\right|^2 g(b,k_1)\Phi_{vv}(k_1)$$

In this expression everything else is known or measured except $g(b,k_1)$. Actually, nothing has been gained so far, because calculation of $g(b,k_1)$ requires information regarding the two-dimensional turbulence spectrum $\tilde{\Phi}(k_1,k_2)$. However, $g(b,k)$ contains only integrals of the spectrum and consequently may not depend too much on the exact expression for $\tilde{\Phi}_{vv}(k_1,k_2)$. The possibility of using a simplified expression for computation of $g(b,k_1)$ becomes apparent; even then, however, some connection must be retained to the actual measured spectrum through one or more free parameters.

Experimental results (for instance, refs. 23 and 24) indicate that grid turbulence can be reasonably described by a simple spectrum which, assuming homogeneity and isotropy, leads to the following form of the two-wave-number power spectrum for the fluctuation component normal to the main stream (see also ref. 15):

$$\left(\tilde{\Phi}_{vv}\right)_o(k_1,k_2) = \frac{3\Lambda^4}{4\pi}\frac{\overline{v^2}\left(k_1^2 + k_2^2\right)}{\left[1 + \Lambda^2\left(k_1^2 + k_2^2\right)\right]^{5/2}}$$

The integral scale Λ, formally the integral over the corresponding normalized correlation function for streamwise fluctuations, represents a characteristic length of the turbulence and is the free parameter to be determined by comparison with the measured spectrum. In this matching, use can be made of the integral

$$\left(\Phi_{vv}\right)_o(k_1) = \int_{-\infty}^{\infty}\left(\tilde{\Phi}_{vv}\right)_o(k_1,k_2)dk_2 = \frac{\Lambda}{2\pi}\frac{\overline{v^2}\left(1 + 3\Lambda^2k_1^2\right)}{\left(1 + \Lambda^2k_1^2\right)^2}$$

which can be compared directly with the measured $\Phi_{vv}(k_1)$.

Substitution of $\left(\tilde{\Phi}_{vv}\right)_o$ into the expression for $g\left(b,k_1\right)$ yields finally

$$g\left(b,k_1,\Lambda\right) = \frac{1}{1 + 3\beta^2}\left[\left(1 - 3\beta^2\right)\frac{1 - 2\epsilon K_1(2\epsilon)}{\epsilon^2} - 2K_o(2\epsilon) + \frac{6\beta^2}{\epsilon}\int_0^{\epsilon} K_o(2\epsilon')d\epsilon'\right]$$

where K_o and K_1 are modified Bessel functions of the second kind and

$$\epsilon = \frac{b}{2\Lambda}\sqrt{1 + \Lambda^2 k_1^2}$$

$$\beta = \Lambda k_1$$

A graphical presentation of $g\left(b,k_1,\Lambda\right)$ is best given in terms of the dimensionless parameters Λ/b and $\frac{b}{c}k = \frac{bk_1}{2}$. Such a plot is presented in figure 27, while figure 24 gives the complete transfer function $\left|S(k)\right|^2 g\left(b,\frac{2k}{c},\Lambda\right)$ for the present experimental configuration at $\Lambda/b = 1$ and 1/2. It should be noted that even if $\Lambda/b \to \infty$, Sears' function is obtained as a limiting case for all values of k only when $b/c \to 0$, that is, for an infinitely narrow strip.

It can also be shown that, for small values of b, $g\left(b,k_1,\Lambda\right)$ can be expressed in power series as

$$g = 1 - \text{Constant} \times b^2 + \ldots \qquad (b \ll \Lambda)$$

Thus, the power spectral density and its integral, the mean-square lift, are proportional to the square of the wing area for small values of span. This result is in accordance with the general behavior of linear systems responding to turbulent excitation. For high values of b/Λ, however, one obtains the following asymptotic expression:

$$g\left(b,k_1,\Lambda\right) = \frac{1}{1 + 3\Lambda^2 k_1^2}\left[\frac{1 - 3\Lambda^2 k_1^2}{\left(\frac{b}{2\Lambda}\right)^2\left(1 + \Lambda^2 k_1^2\right)} + \frac{3\pi\Lambda^2 k_1^2}{\left(\frac{b}{\Lambda}\right)\sqrt{1 + \Lambda^2 k_1^2}}\right] \qquad \left(\frac{b}{\Lambda} \to \infty\right)$$

This means that for large-span wings at low wave numbers, the span correction behaves proportionally to $1/b^2$, whereas at high wave numbers it becomes approximately $1/b$. If one then considers the lift power spectrum, which includes a factor b^2 in the square of the wing area (the Sears' function also included is independent of b), the mean-square total lift can be integrated in the form

$$\overline{L^2} \rightarrow F_1\left(\frac{c}{\Lambda}\right) + F_2\left(\frac{c}{\Lambda}\right)b \qquad (b \rightarrow \infty)$$

where $F_1, F_2 \neq 0$.

In summary, if the wing span is increased from zero while keeping all other conditions unchanged, at very small spans the mean-square lift first increases proportionally to the square of the wing area. For large values of the span, the low-frequency part of the lift spectrum approaches asymptotically a constant nonzero value, while the high-frequency part becomes asymptotically proportional to the span. Correspondingly, the asymptotic expression for the total mean-square lift has a constant term and a term proportional to the span.

Discussion of Results

The experimental results obtained in the present investigation are plotted and compared with the corresponding theoretical predictions in figure 24. As pointed out previously, the turbulence scale Λ appearing in the derivation of the span correction factor g should be determined on the basis of the measured one-wave-number spectrum. Attempts were made to do so; however, since the quantitative values of the power spectrum were doubtful and in any case extended over a limited frequency range, a reliable estimate of Λ could not be obtained in this manner. Dryden, Schubauer, Mock, and Skramstad (ref. 23) have investigated the turbulence scale downstream of coarse grids. If one neglects differences in the shape of grid members and possible effects of the background turbulence in the wind tunnel, the measurements of reference 23 would indicate for the present case a scale roughly 20 to 25 percent of the grid mesh size, that is, Λ = 1.2 to 1.5 inches. This would mean $0.4 < \Lambda/b < 0.5$, which is in good agreement with the experimental results at reduced frequencies above approximately 0.5; at lower frequencies the scatter prevents definite conclusions.

Concurrently with the present investigation, Lamson (ref. 13) has measured the aerodynamic transfer function of an essentially similar configuration. His results cover two turbulence scale-to-span ratios (10/7 and 5/7) and also demonstrate the effect of end plates shielding the measuring element from turbulence along the fixed span. The corresponding theoretical transfer functions, based on the present analysis,

are compared with Lamson's data in figure 28(a) (no end plates) and 28(b) (with end plates). In the former case, agreement in order of magnitude and dependence on turbulence scale-to-span ratio is obtained at $k > 1$. In case of end plates, the analysis could actually be expected to be more accurate in view of the strip-theory assumption; in fact, for $k > 0.8$, Lamson's measurements are now above the theoretical estimates. For lower values of the reduced frequency, the experimental results in both cases fall below the analytical curves and for $k < 0.2$ the dependence on turbulence scale-to-span ratio is actually reversed.

Thus, at high-enough reduced frequencies, the present analysis predicts an order of magnitude and dependence on turbulence scale-to-span ratio in essential agreement with existing experimental evidence. The quantitative difference between the measurements of Lamson and those of the present report may be traceable to factors such as the use of a wing of total aspect ratio 2.8 in an open jet (Lamson) and one of aspect ratio 5 in a closed wind tunnel (present investigation). Also, the method employed by Lamson for determination of turbulence scale is different and actually makes use of measured characteristics of the power spectrum.

It is believed that a more extensive, systematic series of measurements involving several wing configurations is still needed for complete and conclusive evaluation of the validity of the theoretical approach. Such measurements should be accompanied by a detailed investigation of the turbulence in order to determine its scale and to see how well the assumption of the approximate spectrum formula is justified. Analytically, the weakest link appears to be the use of strip theory in the computation of the aerodynamic influence functions; theoretical research on this problem would be very worthwhile.

CONCLUDING REMARKS

Instrumentation for measurement and analysis of downwash and lift fluctuations was developed and found to operate satisfactorily.

Experimental values of Sears' gust function could not be obtained because of excessive scatter of the measurements. The order of magnitude and trend of the measured downwash and lift, however, agreed with theoretical predictions. Conclusive measurements would require improvement in environmental conditions, especially in the background turbulence level of the wind tunnel.

Measurements were made of the transfer function between the power spectra of random downwash and the lift produced thereby on a simple rigid airfoil. An approximate theoretical result was also derived and

compared with the present measurements as well as with those of another investigation. Reasonable agreement was obtained at high reduced frequencies. Further experiments are recommended in order to evaluate completely the validity of the theoretical approach. Improvements in the theoretical treatment would also be desirable, especially in regard to the aerodynamic influence functions.

Massachusetts Institute of Technology,
Cambridge, Mass., July 1, 1955.

APPENDIX A

OPERATION OF X-WIRE HOT-WIRE PROBE FOR CROSS-VELOCITY MEASUREMENT

The customary practical representation of the response characteristics of an oblique hot-wire is based on Kings' law combined with the assumption that the wire responds only to the velocity component normal to it. (See sketch and, for instance, ref. 25.)

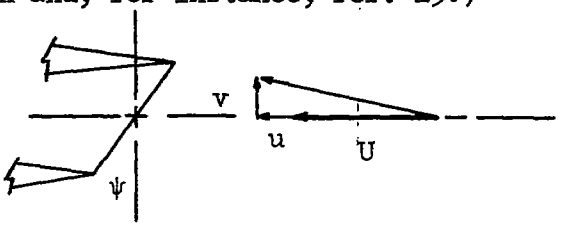

The resulting mathematical expression is

$$I^2 = I_o^2 \frac{2a_w'}{1 + a_w'}\left(\sqrt{\frac{U \cos \psi}{U_o}} + 1\right) \tag{A1}$$

where I_o and U_o are calibration constants, I is the heating current, U is the velocity, ψ is the sweep angle, and $a_w' = \left(R_w - R_e\right)/R_e$, the overheat factor or the relative resistance increase due to heating of the wire. In terms of the current I and cold resistance R_e, the voltage output ν of the wire can be expressed

$$\nu = \frac{IR_e}{1 - \frac{I^2}{2I_o^2}\left(\frac{1}{\sqrt{\frac{U \cos \psi}{U_o}} + 1}\right)} \tag{A2}$$

If the velocity is perturbed slightly by disturbance components u and v, the linearized perturbation in ν will be

$$\Delta v = \frac{I_o^2 R_e}{I^2 U} \frac{1 + \sqrt{\frac{U \cos \psi}{U_o}}}{\left(1 + \sqrt{\frac{U_o}{U \cos \psi}}\right)\left[1 - 2\frac{I_o^2}{I^2}\left(1 + \sqrt{\frac{U \cos \psi}{U_o}}\right)\right]^2}\left(u + \frac{v}{\cot \psi}\right)$$

$$= Cu + Dv \tag{A3}$$

provided that current I is kept constant, which is the case in the present hot-wire circuit.

In an x-probe, another wire is placed at an angle of approximately $-\psi$ with respect to the flow. If one now combines the outputs of the two wires as follows, applying a voltage stepdown device with factor r to one wire, the total response is

$$\begin{aligned} \Delta v_{1,2} &= \Delta v_1 - \Delta v_2 \\ &= \left(C_1 u + D_1 v\right) - r\left(C_2 u - D_2 v\right) \\ &= \left(C_1 - rC_2\right)u + \left(D_1 + rD_2\right)v \end{aligned} \tag{A4}$$

If the wires and their operating conditions were exactly identical, one would have $C_1 = C_2$, and with no voltage stepdown ($r = 1$) the probe would respond to v-fluctuation only.

Generally, it is not possible to produce two wires with exactly identical calibration constants. However, even in that case, the factor $C_1 - rC_2$ can be made equal to zero independently of the mean velocity U by suitable choice of the heating currents, the probe orientation with respect to the mean flow, and the stepdown ratio r. By examination of equations (A3) and (A4), one can write the following conditions:

Heating-current ratio,

$$\frac{I_1}{I_2} = \frac{(I_o)_1}{(I_o)_2} \tag{A5}$$

stepdown factor,

$$r = \frac{(I_o)_1 (R_e)_1}{(I_o)_2 (R_e)_2} \tag{A6}$$

and probe orientation,

$$\frac{\cos \psi_1}{\cos \psi_2} = \frac{(U_o)_1}{(U_o)_2} \tag{A7}$$

where $\psi_1 + \psi_2$ is constant.

The calibration constants I_o and R_e can be readily obtained in the form of equation (A1) from static calibrations of the individual wires, thus making possible the fulfillment of the first two conditions. The third one implies knowledge of the total angle between the two hot-wires. There is, however, no need to perform elaborate precision measurements and adjustments of the probe because the fulfillment of the three conditions (eqs. (A5) to (A7)) also make the total direct-current output $v_{1,2}$ of the two-wire combination equal to zero, as can easily be seen in the following equation:

$$v_{1,2} = v_1 - rv_2 = \frac{I_1(R_e)_1}{1 - \frac{I_1^2}{2(I_o)_1^2}\left(\frac{1}{\sqrt{\frac{U \cos \psi_1}{(U_o)_1}} + 1}\right)} - \frac{rI_2(R_e)_2}{1 - \frac{I_2^2}{2(I_o)_2^2}\left(\frac{1}{\sqrt{\frac{U \cos \psi_2}{(U_o)_2}} + 1}\right)} \tag{A8}$$

Thus, one need only to adjust the heating currents and the stepdown voltage divider to satisfy equations (A5) and (A6); thereafter, the third condition (eq. (A7)) can be satisfied by turning the probe relative to the main velocity direction (i.e., by varying ψ_1 and ψ_2) until such a position is found where the total direct-current output (eq. (A8)) vanishes.

This procedure was successfully followed in practice. After adjustments of the probe were completed, its sensitivity to streamwise u-fluctuations was checked by varying the tunnel speed. Generally, the response to a u-disturbance was found to be at most a few percent of the response to a v-disturbance of the same magnitude.

APPENDIX B

STATISTICAL RELIABILITY OF POWER-SPECTRUM MEASUREMENTS

Since it is impossible to measure in practice the infinite time average implied by the use of generalized harmonic analysis, determination of sufficient observation time to obtain values of power spectral density with a specified statistical reliability poses an important problem. In general, the observation time has to be large compared with any characteristic times of the random process. However, since these quantities are themselves objects of measurement, being involved as parameters in the power spectrum or correlation functions, one has to resort to assumptions regarding the probable shape of the power spectrum.

Tukey (ref. 26) considered the accuracy of power spectra computed from a discrete set of sample points of the random function, including different spectrum shapes. The present analysis deals with the reliability of continuous mean-square measurements of the output of a narrow-band-pass filter subjected to the random input and is based on the line of thought presented by Rice (ref. 7). Davenport, Johnson, and Middleton (ref. 27) discuss the same problem employing assumptions somewhat different from those of the present investigation.

It is assumed that (1) the power spectral density to be measured is constant over the filter range; (2) the random process is Gaussian; (3) the band-pass filter is approximately a single tuned circuit with response

$$\left|a\left(\omega,\omega_0\right)\right|^2 = \frac{1}{1 + 4Q^2\left(\frac{\omega - \omega_0}{\omega_0}\right)^2}$$

(4) the squaring device is a heater-thermocouple unit with time lag; and (5) the averaging is done by direct integration of the squared signal.

Let $f(t)$ represent the filter output; then, the thermocouple output is

$$s(t) = \frac{1}{T_c}\int_{-\infty}^{t} e^{\frac{t'-t}{T_c}} f^2(t')dt'$$

where T_c is the time constant of the thermocouple. The infinite time average of s is $\bar{s} = \overline{f^2}$ (ref. 7), while measurement over time T yields

$$\tilde{s} = \frac{1}{T}\int_0^T s(t)dt = \frac{1}{T}\int_0^T \frac{1}{T_c}\left(\int_{-\infty}^{t} e^{\frac{t'-t}{T_c}} f^2(t')dt'\right)dt$$

It is desired to determined the variance of $\tilde{s}$, that is, the quantity

$$\sigma^2 = \overline{\left(\frac{\tilde{s} - \bar{s}}{\bar{s}}\right)^2} = \frac{\overline{\tilde{s}^2}}{\bar{s}^2} - 1$$

Now,

$$\overline{\tilde{s}^2} = \frac{1}{T^2}\iint_0^T \overline{s(t_1)s(t_2)}dt_1\,dt_2 = \frac{2\overline{s^2}}{T^2}\int_0^T (T - \tau)\varphi_{ss}(\tau)d\tau$$

where φ_{ss} is the normalized correlation function of $s(t)$. The product $\overline{s^2}\varphi_{ss}(\tau)$ can be derived from the filter response; by Fourier transform one finds that the normalized correlation function of the filter output is

$$\varphi_{ff}(\tau) = e^{-\frac{\omega_o|\tau|}{2Q}}\cos\omega_o\tau$$

and according to Rice (ref. 7)

$$\overline{s^2}\varphi_s(\tau) = \bar{s}^2\left\{1 + \frac{1}{T_c}\int_0^\infty e^{-\frac{t}{T_c}}\left[\varphi_{ff}^2(t + \tau) + \varphi_{ff}^2(t - \tau)\right]dt\right\}$$

The resulting mathematical expressions become rather lengthy; however, a convenient simplification can be made by assuming that $Q^2 \gg 1$ and $(\omega_o T_c)^2 \gg 1$ which is true in many practical cases. By carrying out the detailed computations and successive substitutions one finally obtains (denoting $\omega_o T/Q = \rho$ and $\omega_o T_c/Q = \gamma$)

$$\sigma = \frac{1}{\rho}\sqrt{\frac{2\gamma\left(1 - \gamma + \gamma e^{-\rho/\gamma} - e^{-\rho}\right)}{1 - \gamma^2}}$$

In the present investigation $Q = 80$, $T_c = 5$ seconds, and $3 < \frac{\omega_o}{2\pi} < 150$ cps; hence, approximately,

$$1 < \gamma < 50$$

Curves of $\sigma(\rho)$ are plotted in figure 25 for $\gamma = 1$, 10, and 50. It is seen that, for example, statistical accuracy of 3 percent root mean square implies the use of integration times of the order $\rho = 50$, that is, from 5 seconds at $\omega_o/2\pi = 150$ cps to over 3 minutes at $\omega_o/2\pi = 3$ cps. In practice, these times were exceeded by a substantial margin to make some allowance for deviations from the assumptions employed in the analysis. It is to be emphasized, however, that the 3 percent is the root-mean-square error of an infinite ensemble of measurements and, therefore, it is impossible to guarantee the accuracy of an individual measurement within specified limits.

Some comment may be in order regarding the curves presented in figure 25. At a low value of ρ the error decreases with increasing time lag γ, which is consistent with physical intuition about the effects of smoothing; however, at higher values of ρ the trend is reversed. The reason for this can be seen by considering the error equation, which may be written

$$\sigma^2 = \frac{2}{T^2}\left(\frac{\overline{s^2}}{\bar{s}^2}\right)\int_0^T (T - \tau)\varphi_{ss}(\tau)d\tau - 1$$

While increasing time lag decreases $\overline{s^2}/\bar{s}^2$ it also makes the fluctuations of s more correlated and thus increases $\varphi_{ss}(\tau)$ in the range of integration. At long integration times, the latter effect becomes dominating.

The values of σ at $\rho = 0$ represent the standard deviation of an instantaneous observation and thus can be employed to estimate the frequency above which integration is no longer necessary.

REFERENCES

1. Doolittle, J. H.: Accelerations in Flight. NACA Rep. 203, 1924.

2. Donely, Philip: Summary of Information Relating to Gust Loads on Airplanes. NACA Rep. 997, 1950. (Formerly NACA TN 1976.)

3. Hislop, G. S.: Clear Air Turbulence Over Europe. Jour. R.A.S., vol. 55, no. 484, Apr. 1951, pp. 185-211.

4. Rhode, Richard V., and Lundquist, Eugene E.: Preliminary Study of Applied Load Factors in Bumpy Air. NACA TN 374, 1931.

5. Küssner, Hans Georg: Beanspruchung von Flugzeugflügeln durch Böen. Z.F.M., Jahrg. 22, Heft 19, Oct. 14, 1931, and Jahrg. 22, Heft 20, Oct. 28, 1931. (Available in English translation as NACA TM 654.)

6. Wiener, Norbert: The Fourier Integral and Certain of Its Applications. The Univ. Press (Cambridge), 1933.

7. Rice, S. O.: Mathematical Analysis of Random Noise. The Bell System Tech. Jour., vol. 23, no. 3, July 1944, pp. 282-332, and vol. 24, no. 1, Jan. 1945, pp. 46-108.

8. Clementson, Gerhardt C.: An Investigation of the Power Spectral Density of Atmospheric Turbulence. Sc. D. Thesis, M.I.T., May 1950.

9. Liepmann, H. W.: An Approach to the Buffeting Problem From Turbulence Considerations. Rep. No. SM-13940, Douglas Aircraft Co., Inc., Mar. 13, 1951.

10. Liepmann, H. W.: On the Application of Statistical Concepts to the Buffeting Problem. Jour. Aero. Sci., vol. 19, no. 12, Dec. 1952, pp. 793-800, 822.

11. Press, Harry, and Mazelsky, Bernard: A Study of the Application of Power-Spectral Methods of Generalized Harmonic Analysis to Gust Loads on Airplanes. NACA Rep. 1172, 1954. (Supersedes NACA TN 2853.)

12. Fung, Y. C.: Statistical Aspect of Dynamic Loads. Jour. Aero. Sci., vol. 20, no. 5, May 1953, pp. 317-330.

13. Lamson, P.: Measurements of Lift Fluctuations Due to Turbulence. NACA TN 3880, 1956.

14. Press, Harry, and Houbolt, John C.: Some Applications of Generalized Harmonic Analysis to Gust Loads of Airplanes. Jour. Aero. Sci., vol. 22, no. 1, Jan. 1955, pp. 17-26, 60.

15. Liepmann, H. W.: Extension of the Statistical Approach to Buffeting and Gust Response of Wings of Finite Span. Jour. Aero. Sci., vol. 22, no. 3, Mar. 1955, pp. 197-200.

16. Diederich, Franklin W.: The Response of an Airplane to Random Atmospheric Disturbances. Ph. D. Thesis, C.I.T., 1954.

17. Richardson, A. S., Jr.: Theoretical and Experimental Investigation of Random Gust Loads. Part II - Theoretical Formulation of Atmospheric Gust Response Problem. NACA TN 3879, 1956.

18. Chippendale, George R., and Clement, Warren F.: The Statistical Study of Atmospheric Turbulence by Flight Measurements. M.S. Thesis, M.I.T., 1951.

19. Summers, Robert A.: A Statistical Description of Large-Scale Atmospheric Turbulence. Sc. D. Thesis, M.I.T., May 1954.

20. Sears, William R.: Some Aspects of Non-Stationary Airfoil Theory and Its Practical Application. Jour. Aero. Sci., vol. 8, no. 3, Jan. 1941, pp. 104-108.

21. Roshko, Anatol: On the Development of Turbulent Wakes From Vortex Streets. NACA Rep. 1191, 1954. (Supersedes NACA TN 2913.)

22. Ashley, Holt: Some Unsteady Aerodynamic Problems Affecting the Dynamic Stability of Aircraft. Sc. D. Thesis, M.I.T., Jan. 1951.

23. Dryden, Hugh L., Schubauer, G. B., Mock, W. C., Jr., and Skramstad, H. K.: Measurements of Intensity and Scale of Wind-Tunnel Turbulence and Their Relation to the Critical Reynolds Number of Spheres. NACA Rep. 581, 1937.

24. Liepmann, H. W., Laufer, J., and Liepmann, Kate: On the Spectrum of Isotropic Turbulence. NACA TN 2473, 1951.

25. Schubauer, G. B., and Klebanoff, P. S.: Theory and Application of Hot-Wire Instruments in the Investigation of Turbulent Boundary Layers. NACA WR-86, 1946. (Formerly NACA ACR 5K27.)

26. Tukey, John W.: The Sampling Theory of Power Spectrum Estimates. Symposium on Applications of Autocorrelation Analysis to Physical Problems (Woods Hole, Mass., June 1949), Office Naval Res., May 1950.

27. Davenport, W. B., Jr., Johnson, R. A., and Middleton, D.: Statistical Errors in Measurements on Random Time Functions. Jour. Appl. Phys., vol. 23, no. 4, Apr. 1952, pp. 377-380.

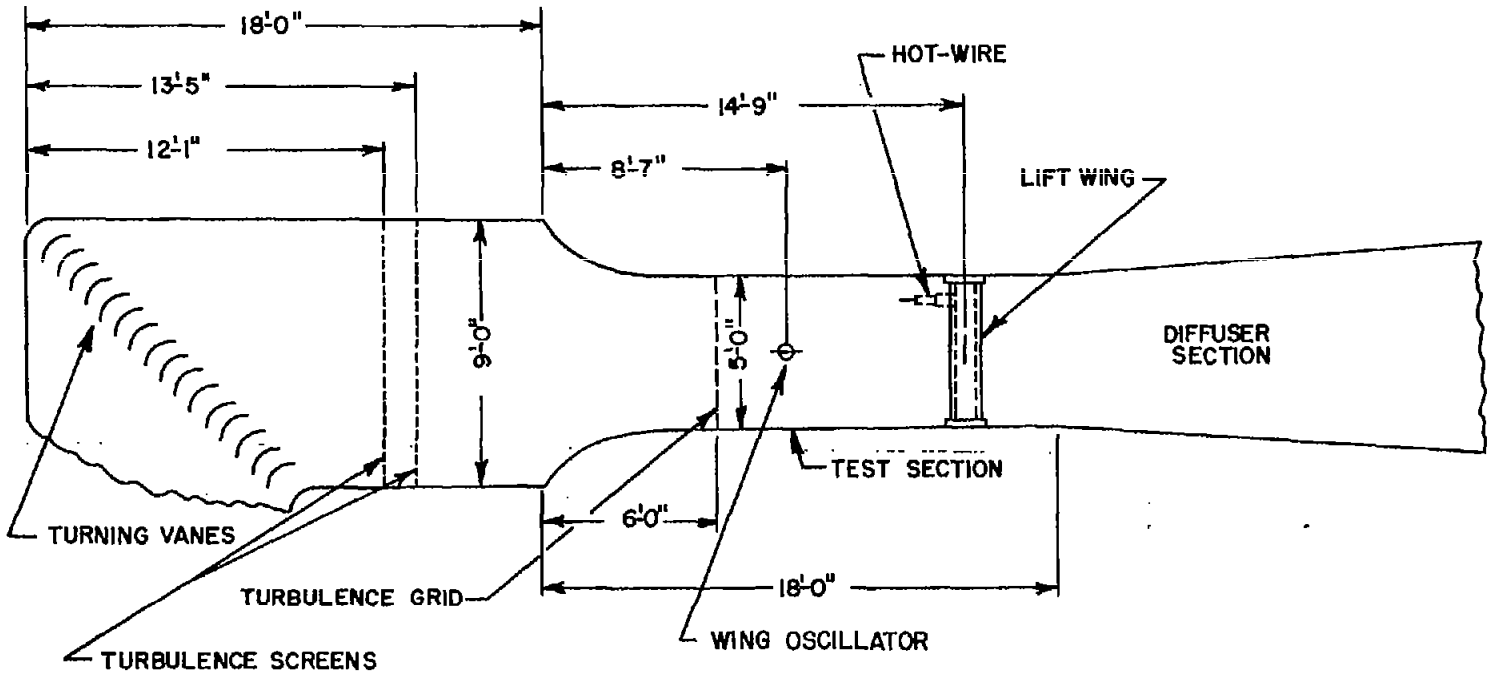

Figure 1.- Side view of 5- by 7.5-foot wind tunnel.

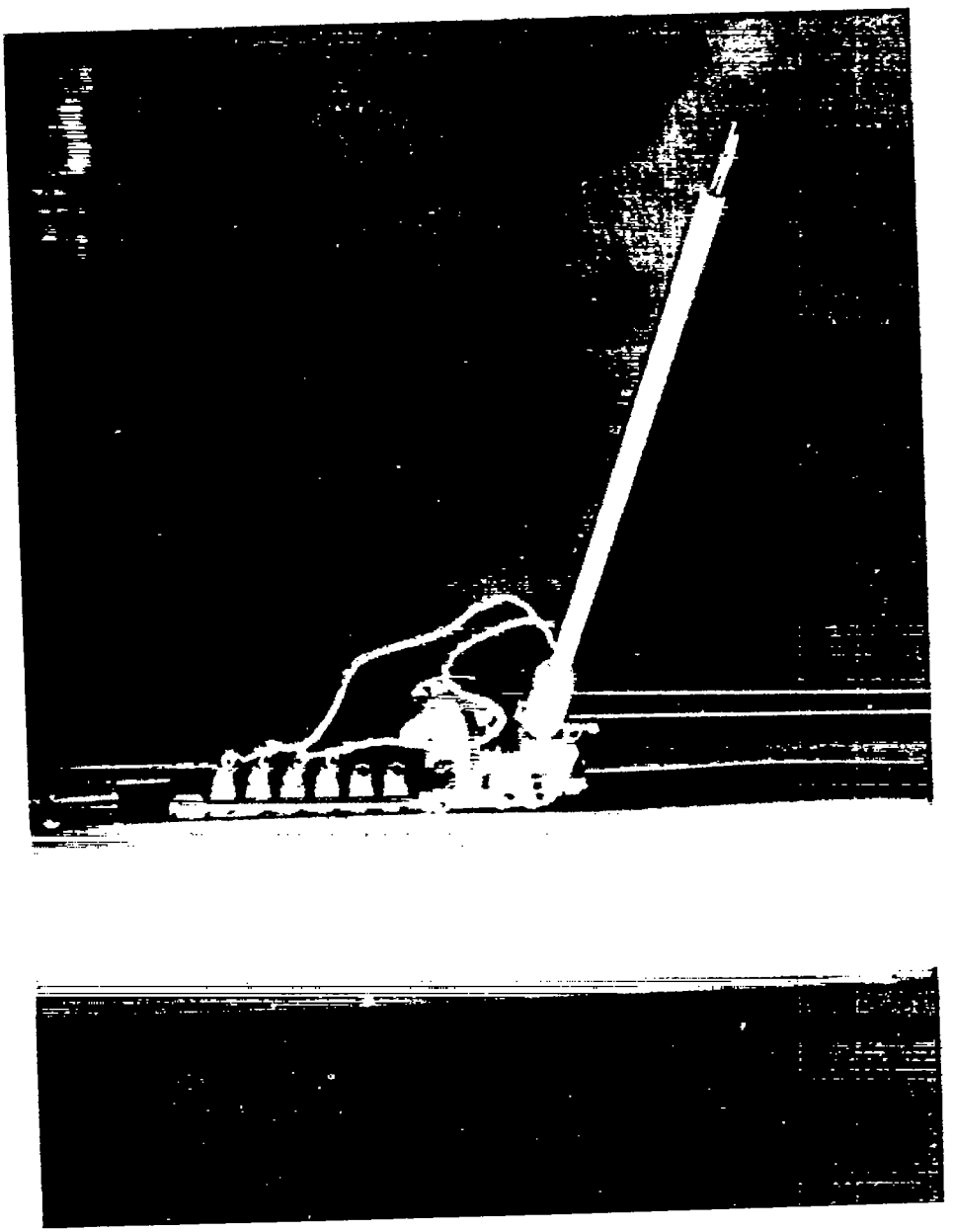

L-95800

Figure 2.- Hot-wire probe.

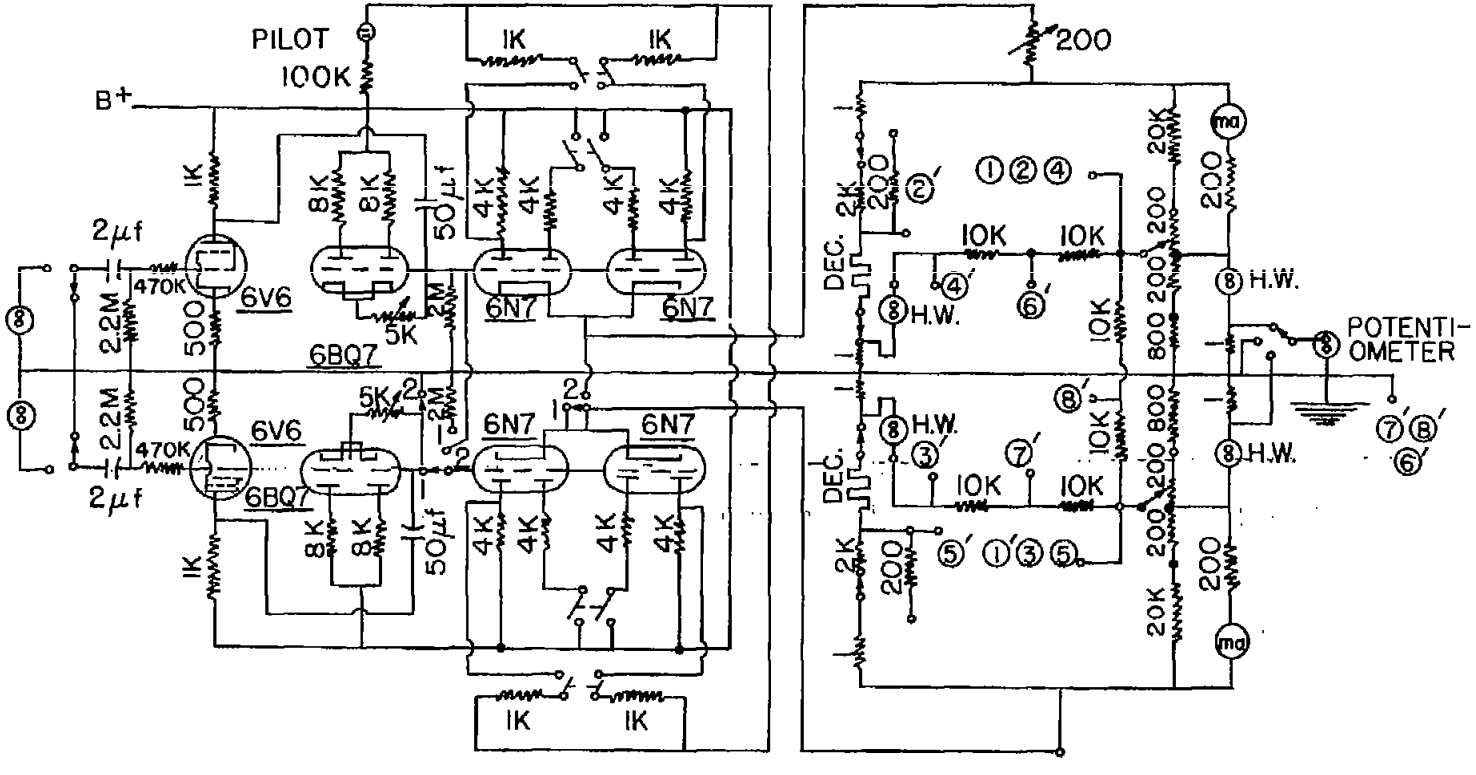

Figure 3.- Hot-wire feeding and bridge circuits. Galvanometer selector, ① - ①′ to ⑤ - ⑤′; amplifier selector, ① - ①′ to ⑧ - ⑧′.

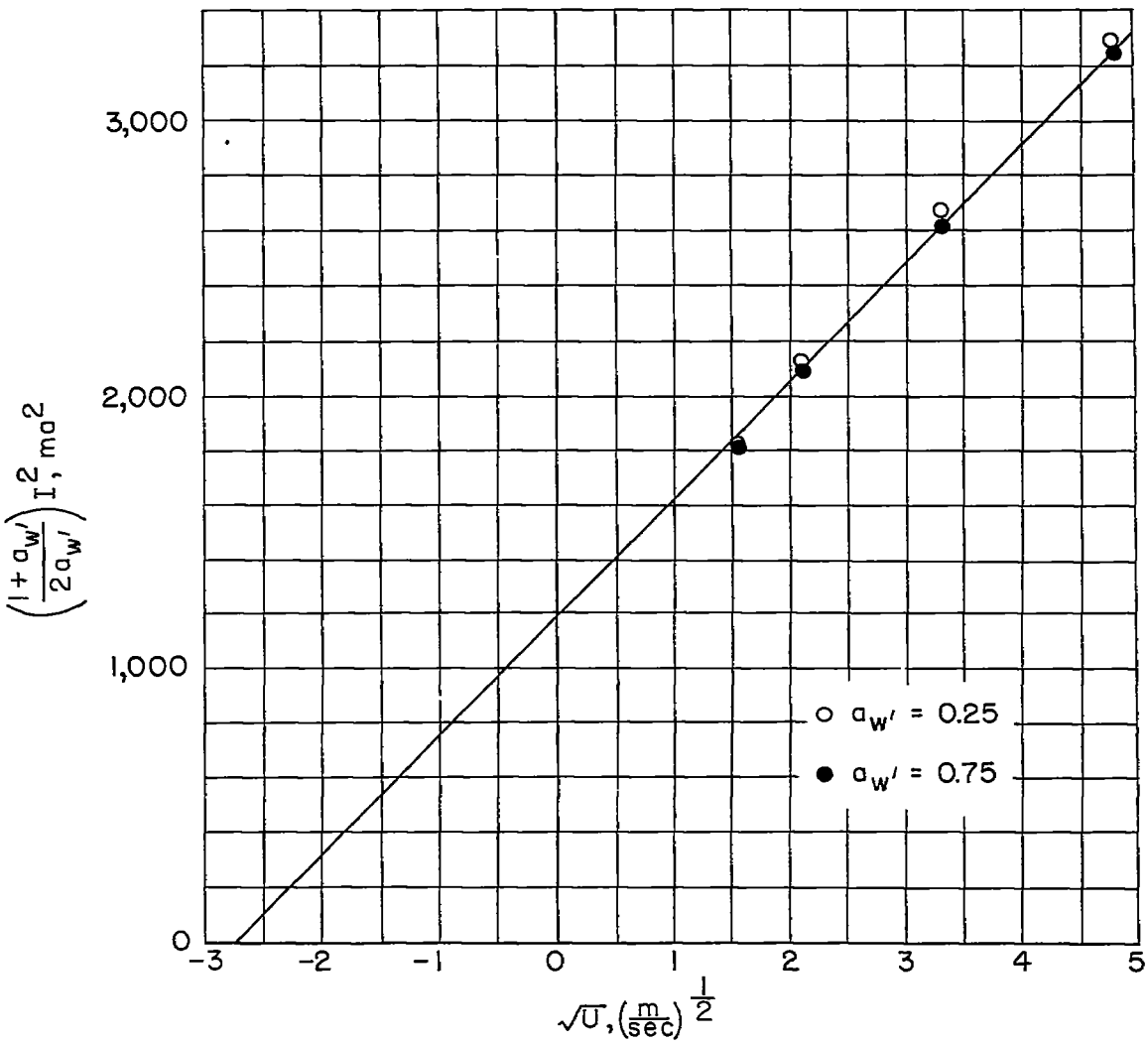

Figure 4.- Typical single hot-wire calibration. $I_o^2 = 1150\ ma^2$.

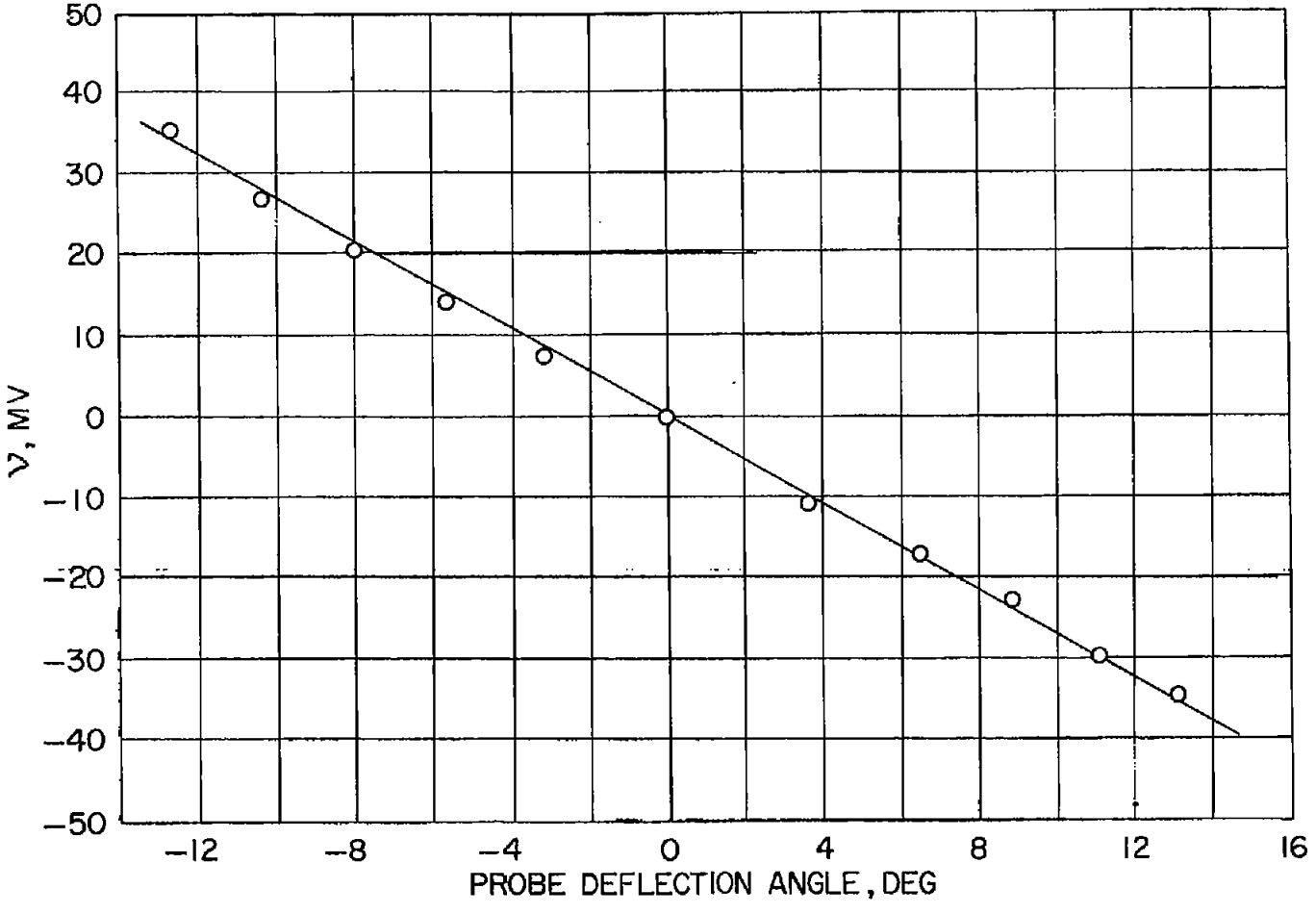

Figure 5.- Typical cross-velocity calibration of double-wire probe. Sensitivity, 2.66 $\frac{mv}{deg}$.

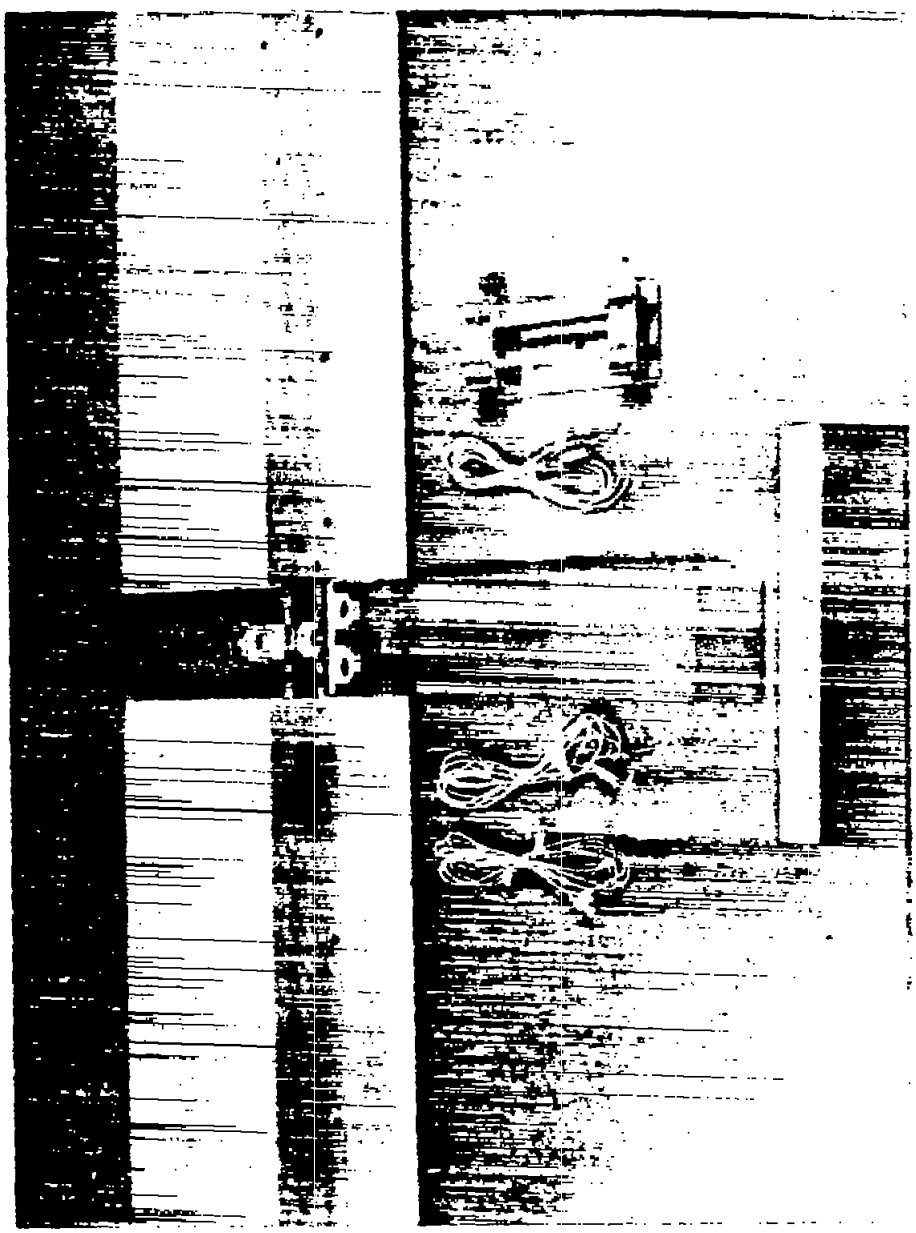

L-95801

Figure 6.- Lift-sensing wing.

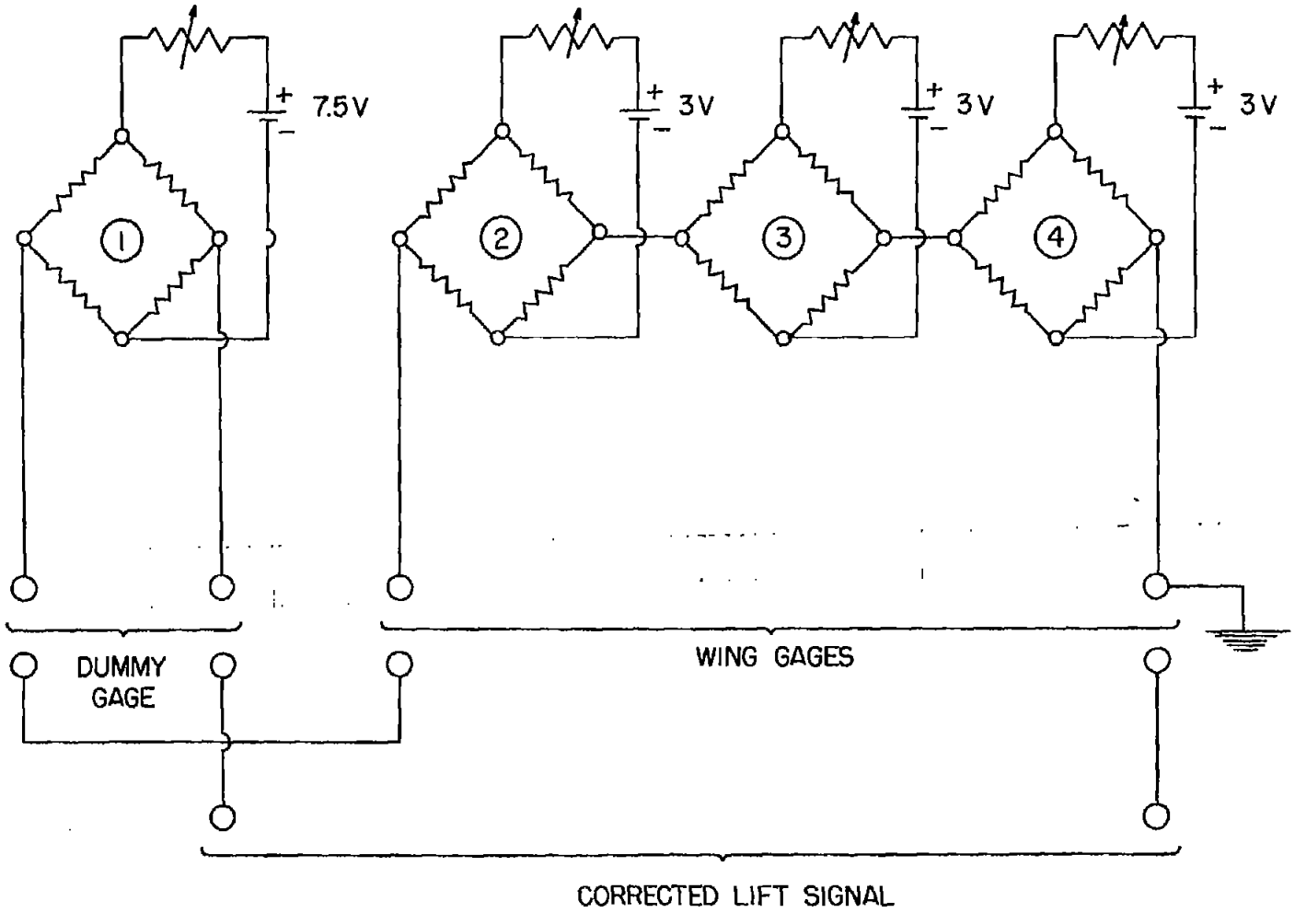

Figure 7.- Circuit diagram of strain-gage force pickups.

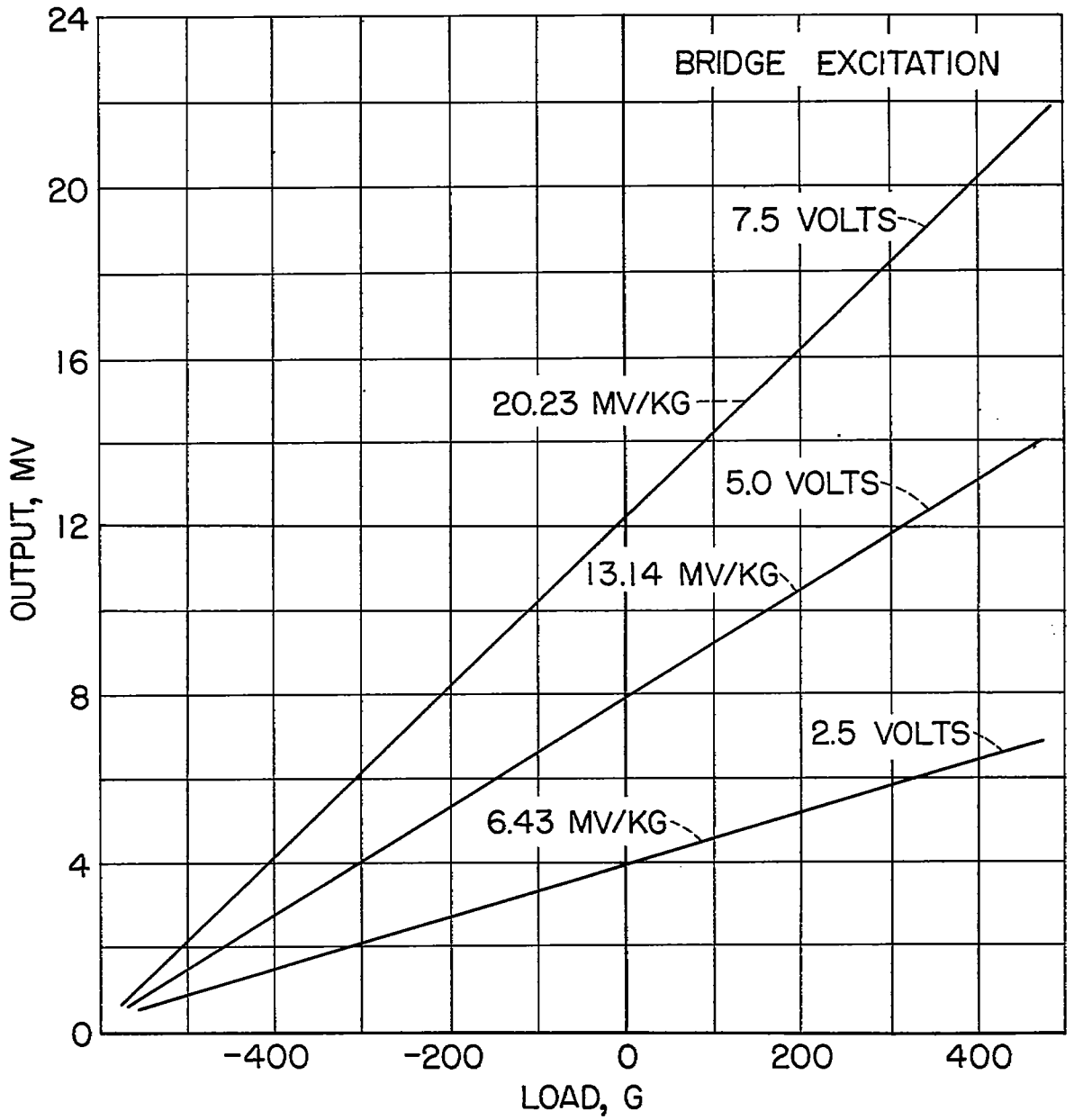

Figure 8.- Static calibration of strain-gage force pickup. Average sensitivity, 2.63 mv/v-kg; maximum deviation, 2.7 percent.

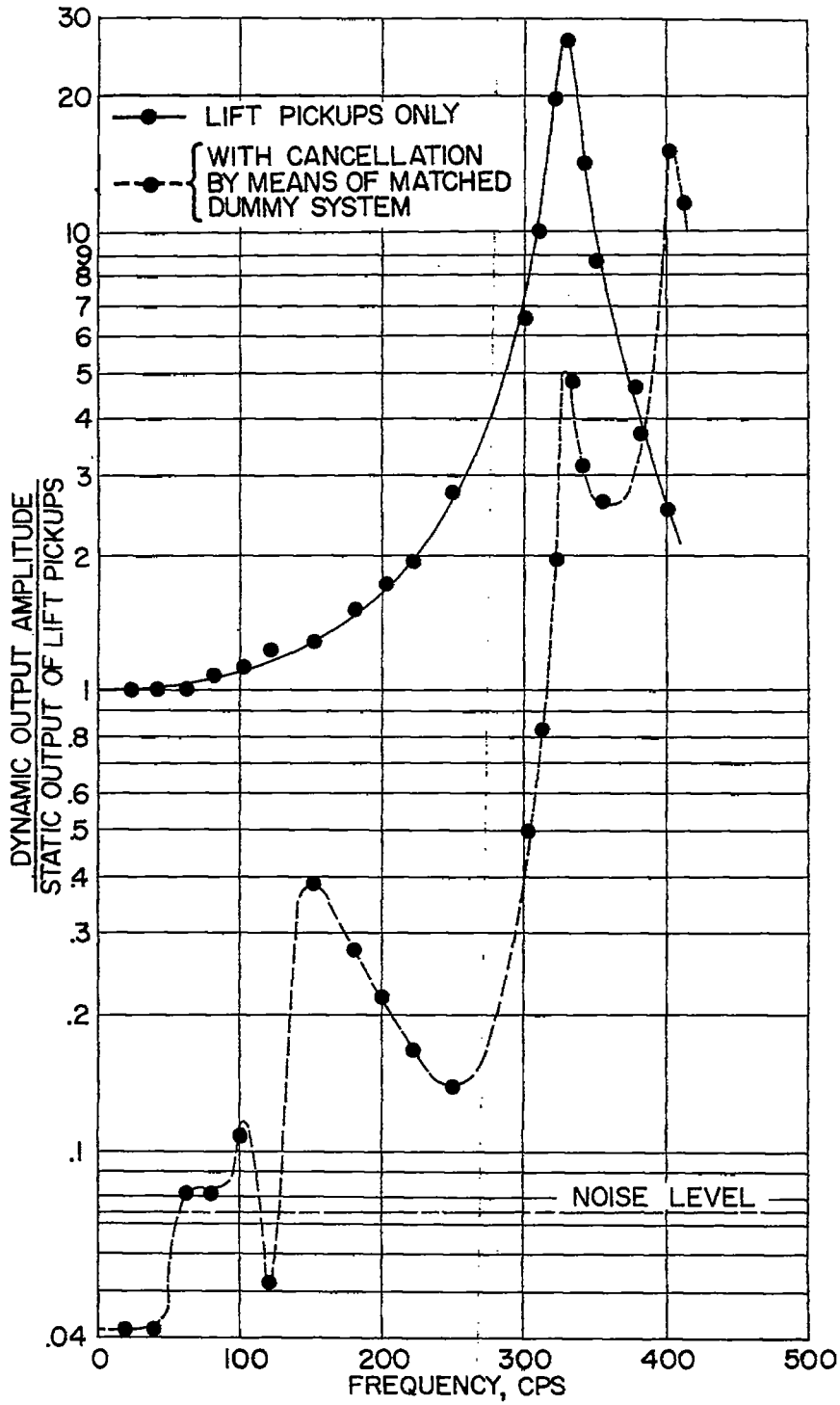

Figure 9.- Dynamic response of lift-pickup system to sinusoidal motion of support at fixed acceleration amplitude.

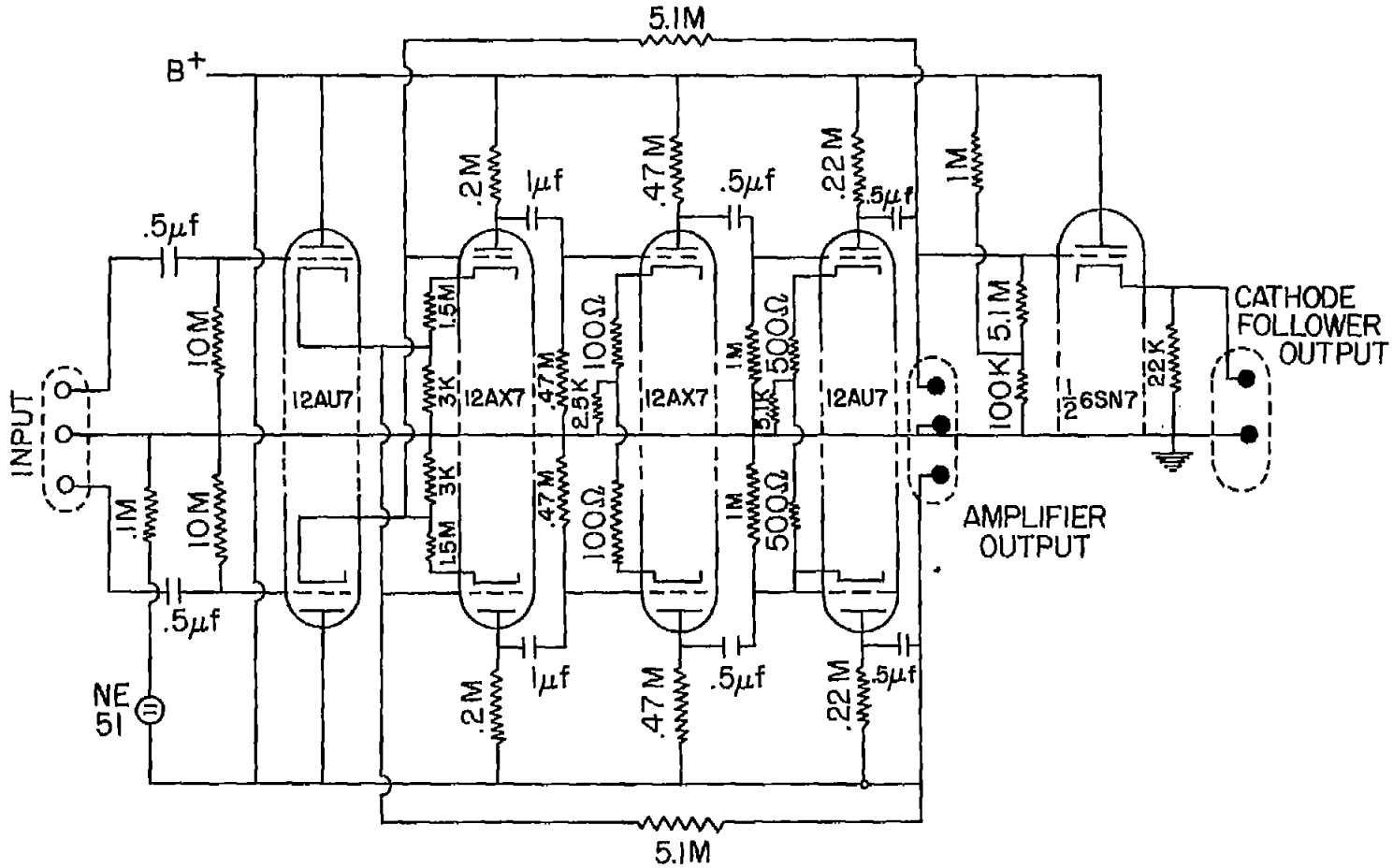

Figure 10.- Amplifier circuit (one channel).

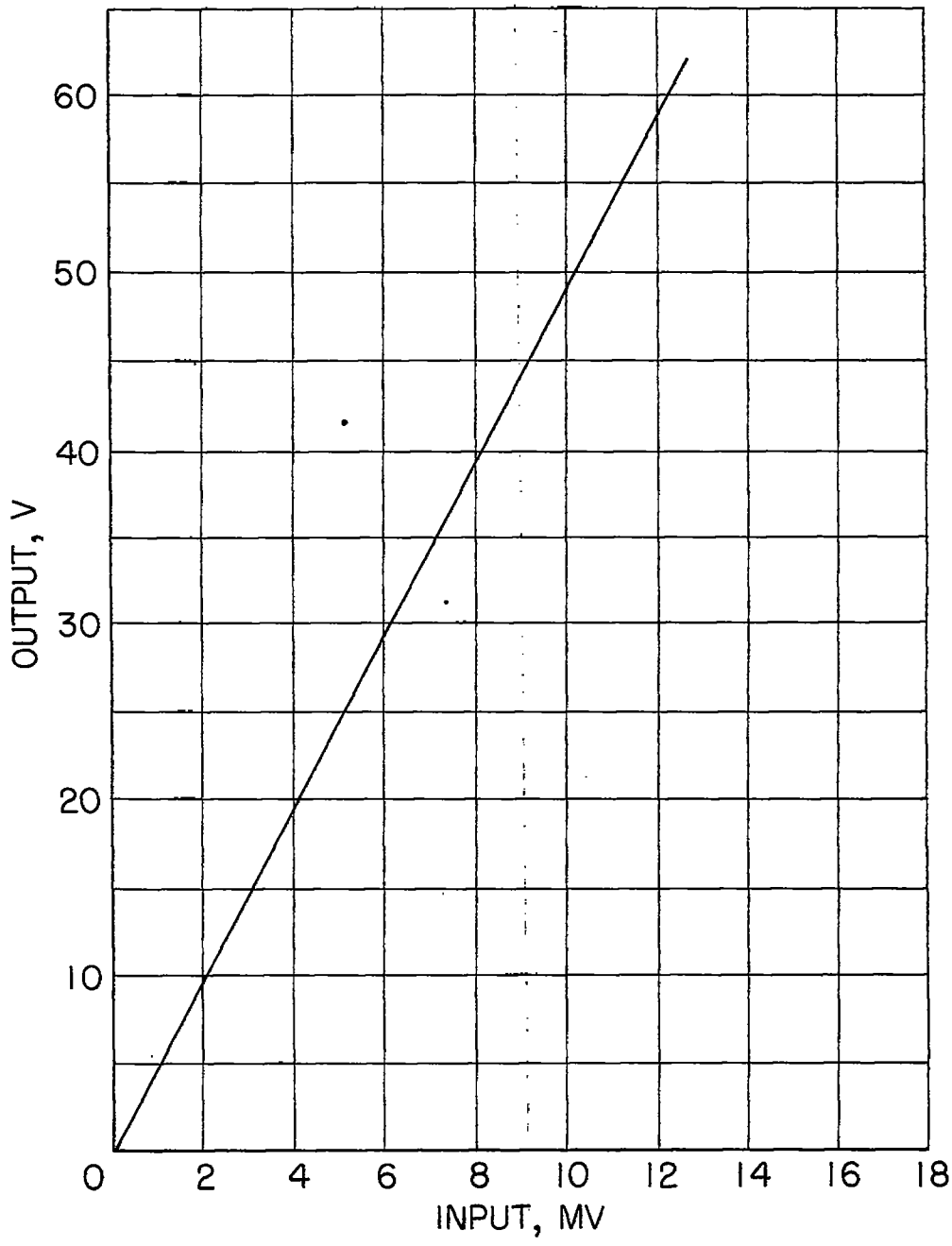

Figure 11.- Calibration of amplifier (push-pull, maximum gain).

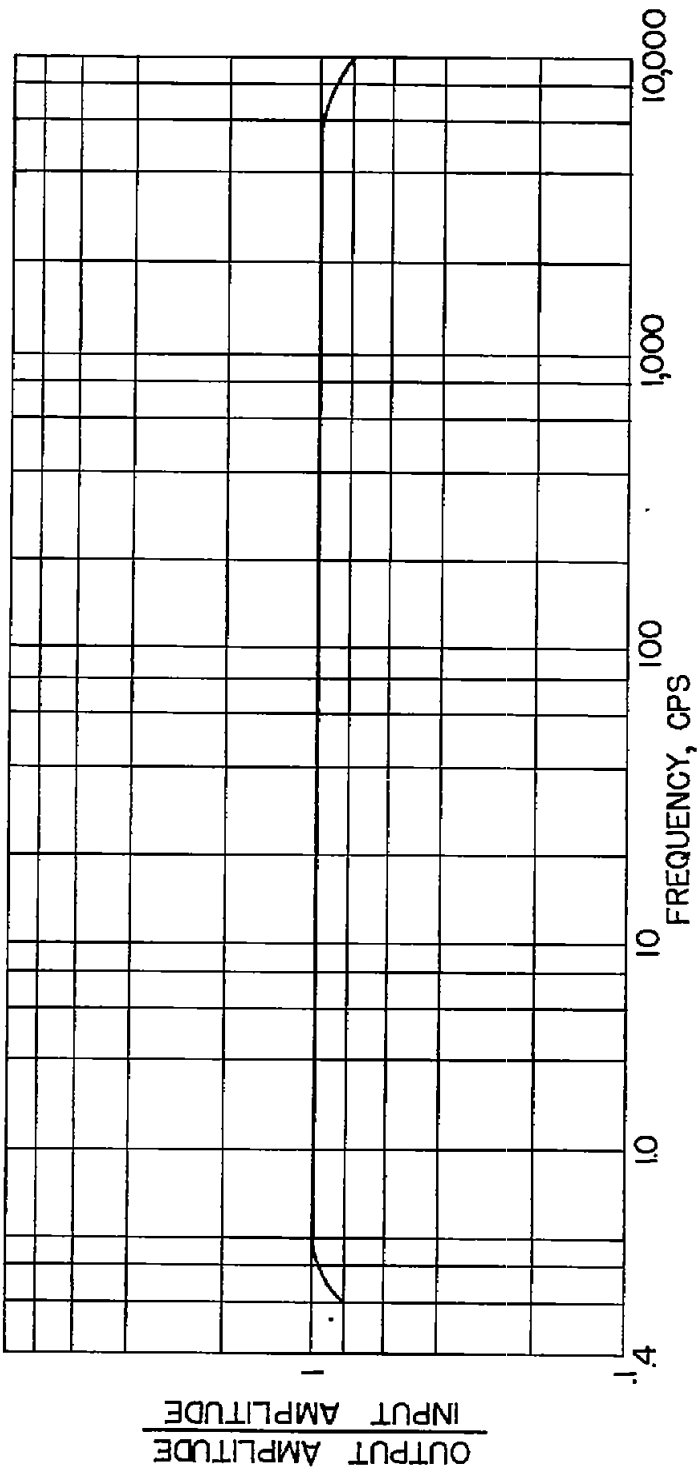

Figure 12.- Frequency response of amplifiers.

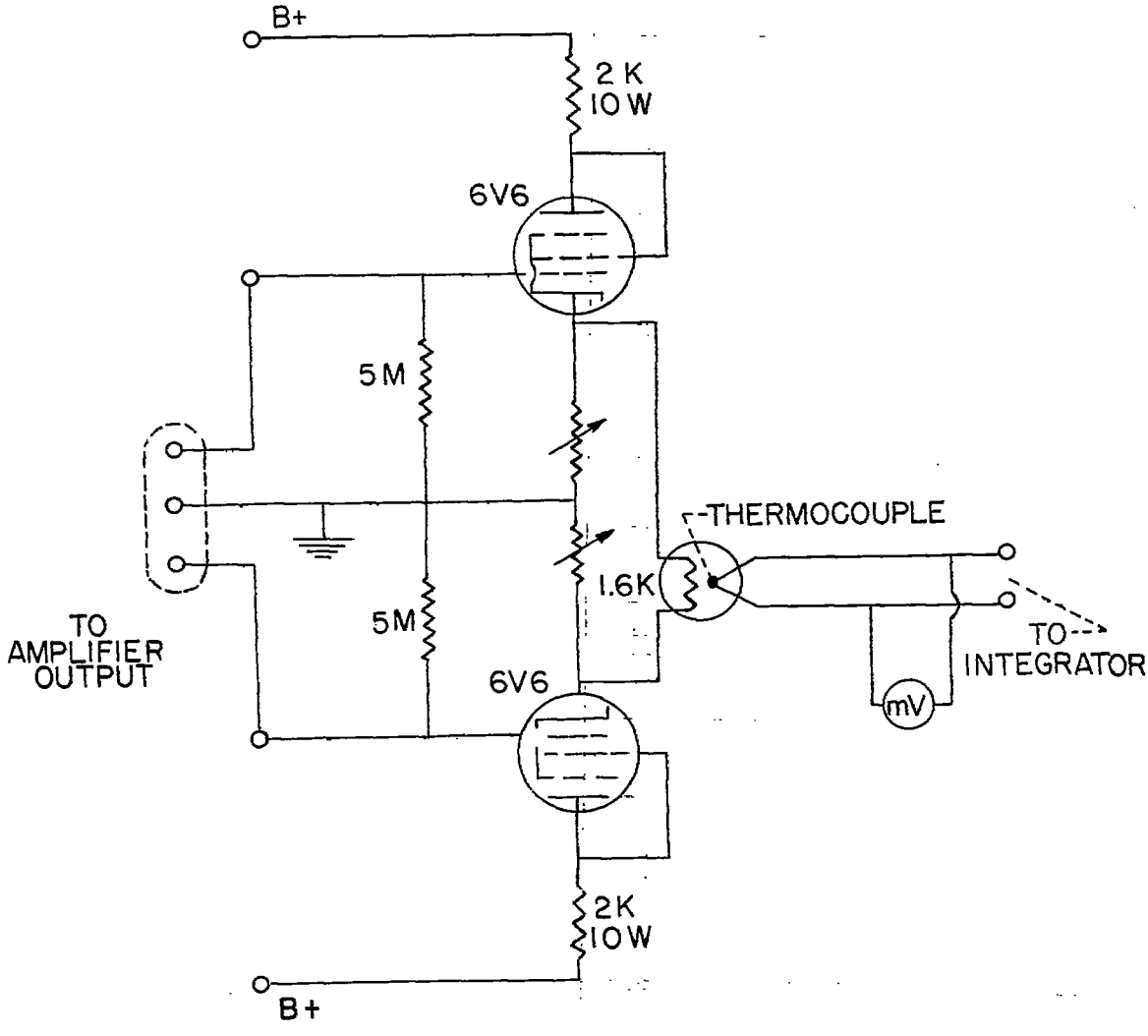

Figure 13.- Circuit for thermocouple driver.

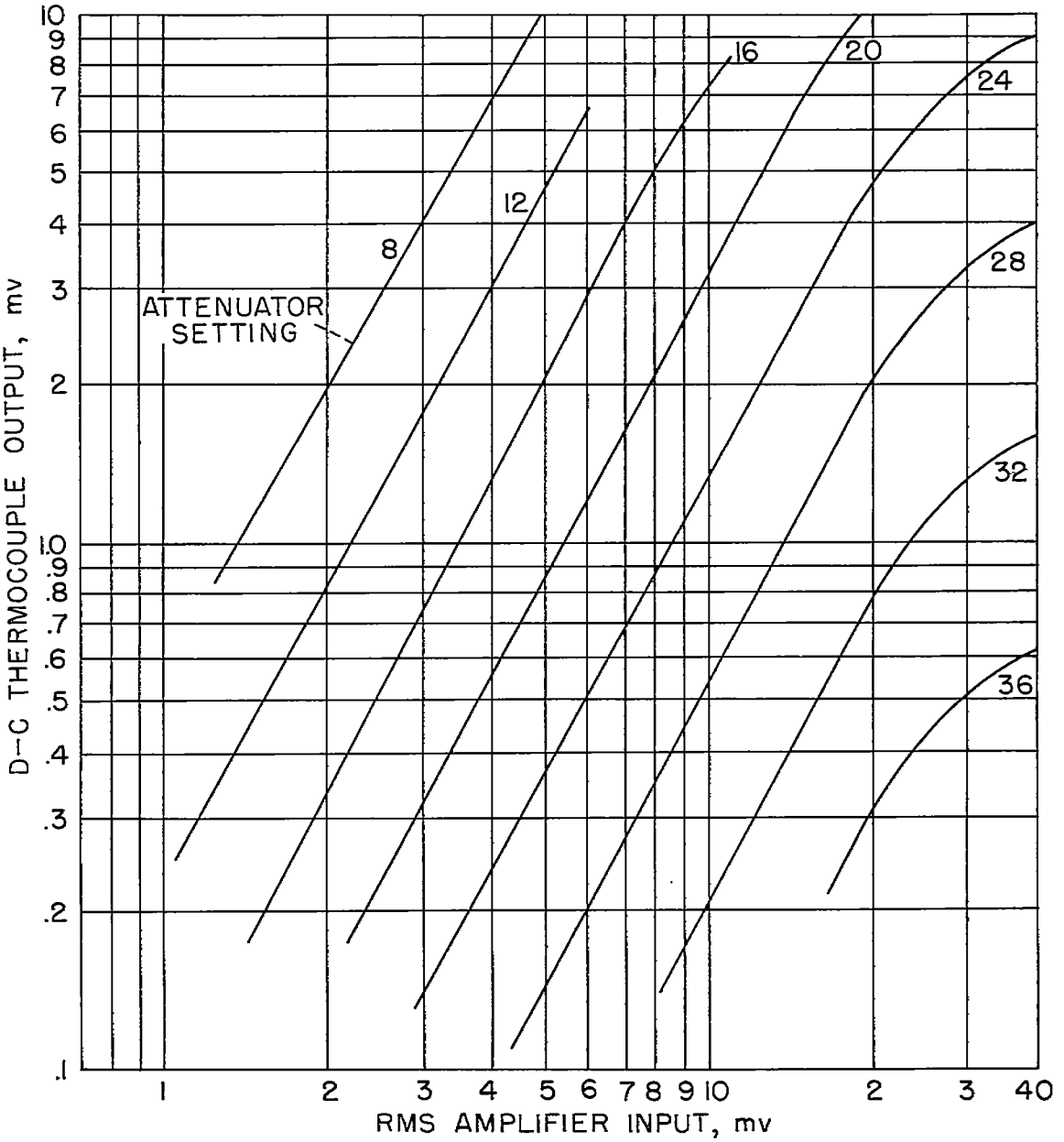

Figure 14.- Thermocouple calibration.

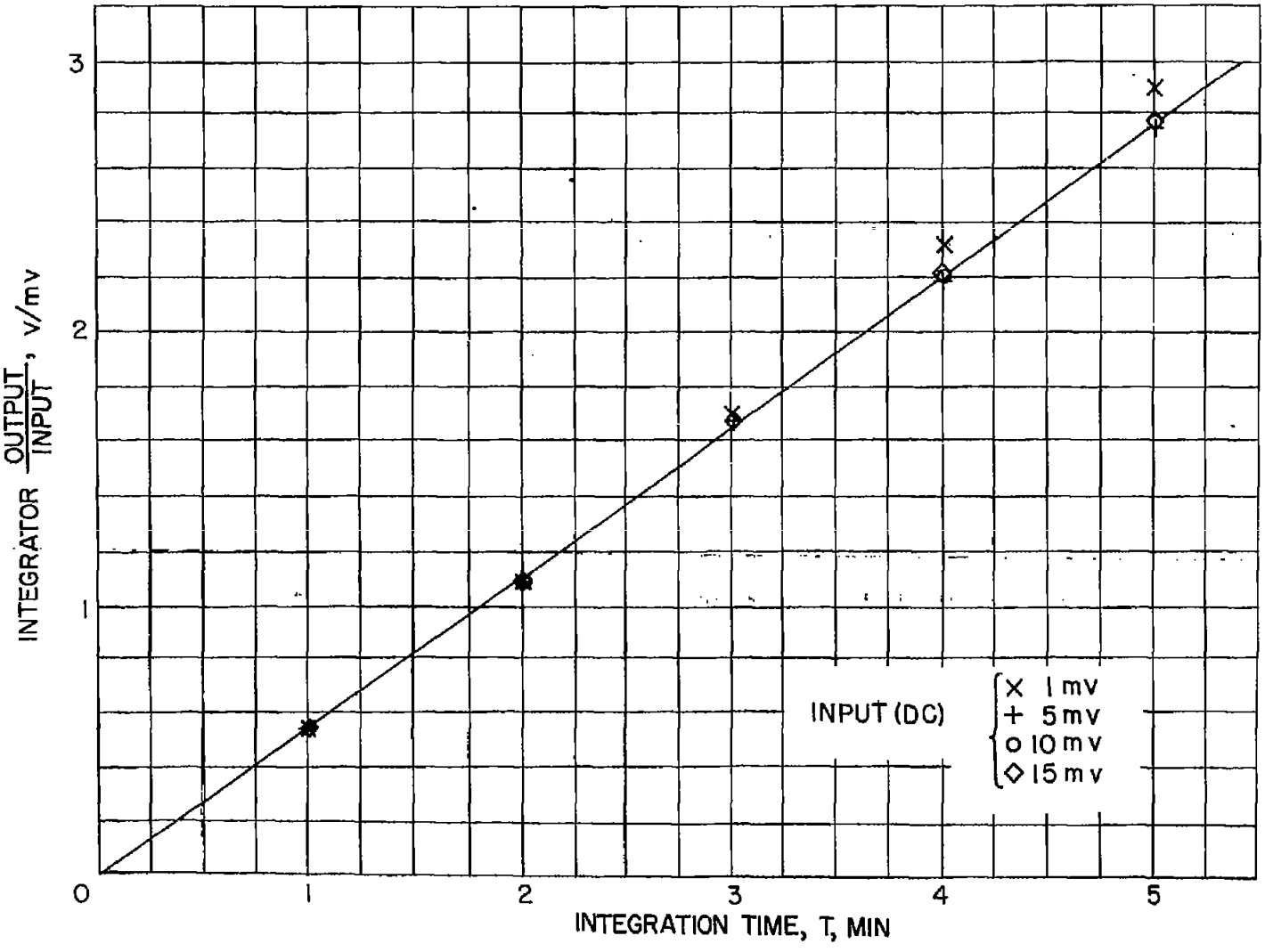

Figure 15.- Integrator calibration. Average slope, 0.556 v/mv-min.

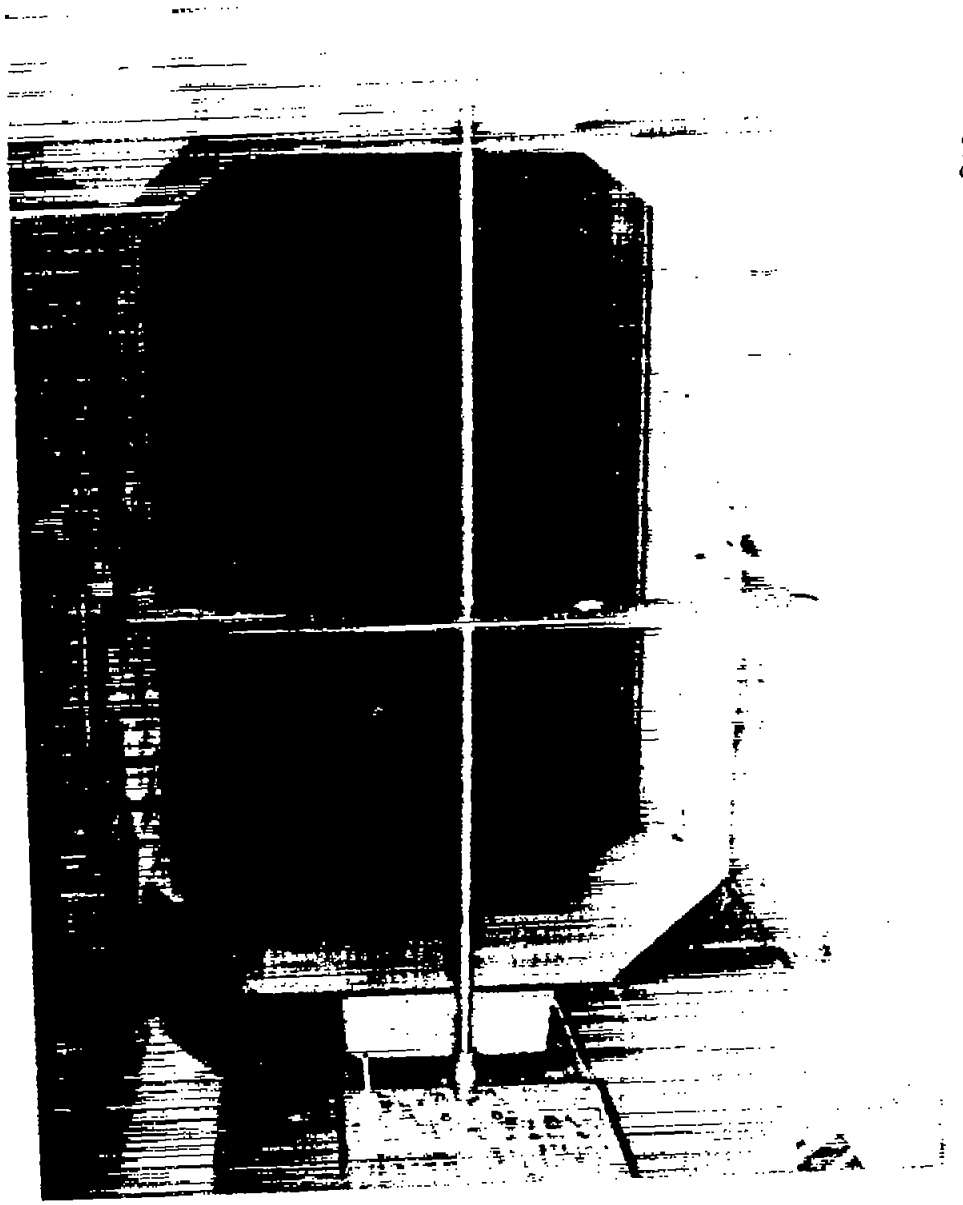

L-95802

Figure 16.- Oscillator wing.

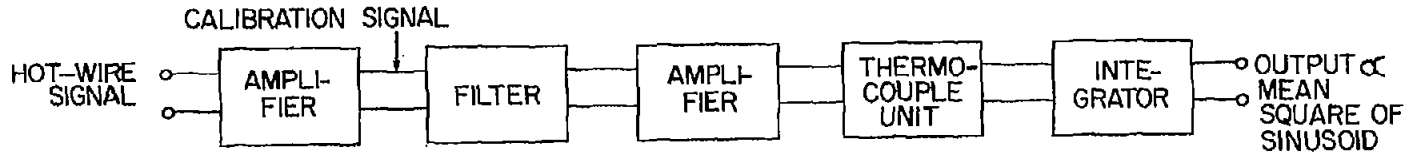

Figure 17.- Block diagram for measurements of sinusoidal downwash.

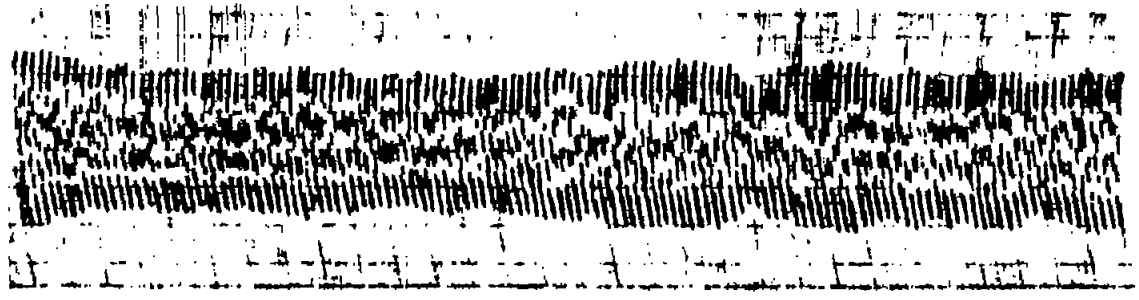

(a) Complete signal.

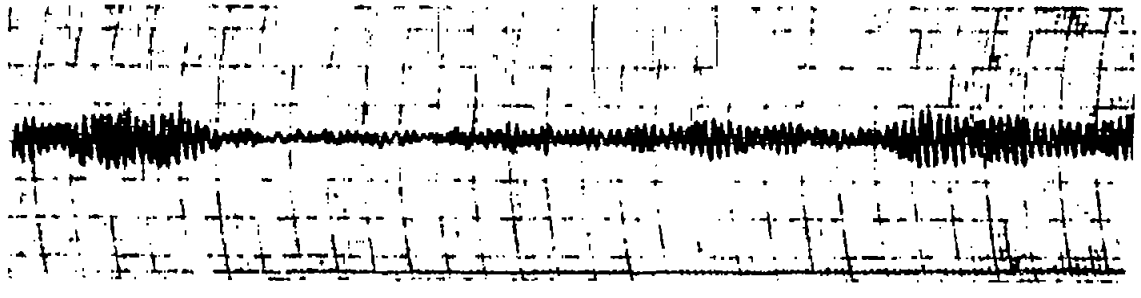

(b) Turbulence and amplifier noise.

Figure 18.- Sample recordings of downwash signal. Frequency, 4.24 cps; recording sensitivity, 70 mm/deg flow deflection.

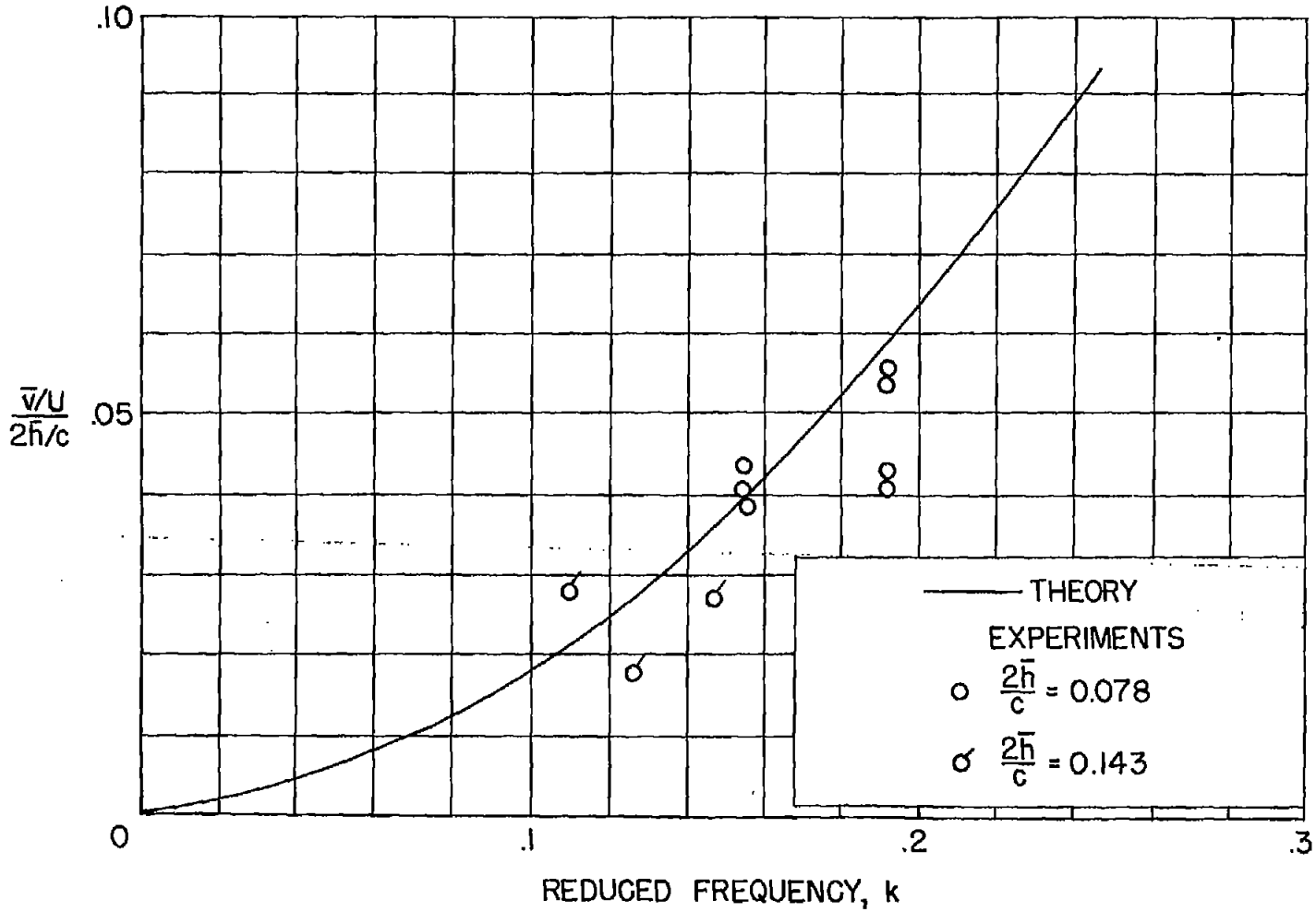

Figure 19.- Measurements of sinusoidal downwash. U = 50 mph.

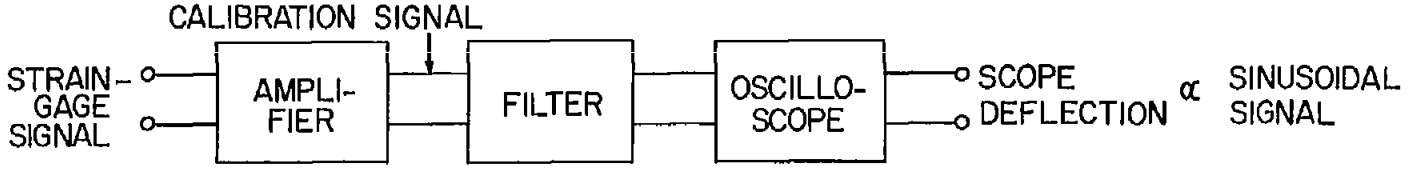

Figure 20.- Block diagram for measurements of sinusoidal lift.

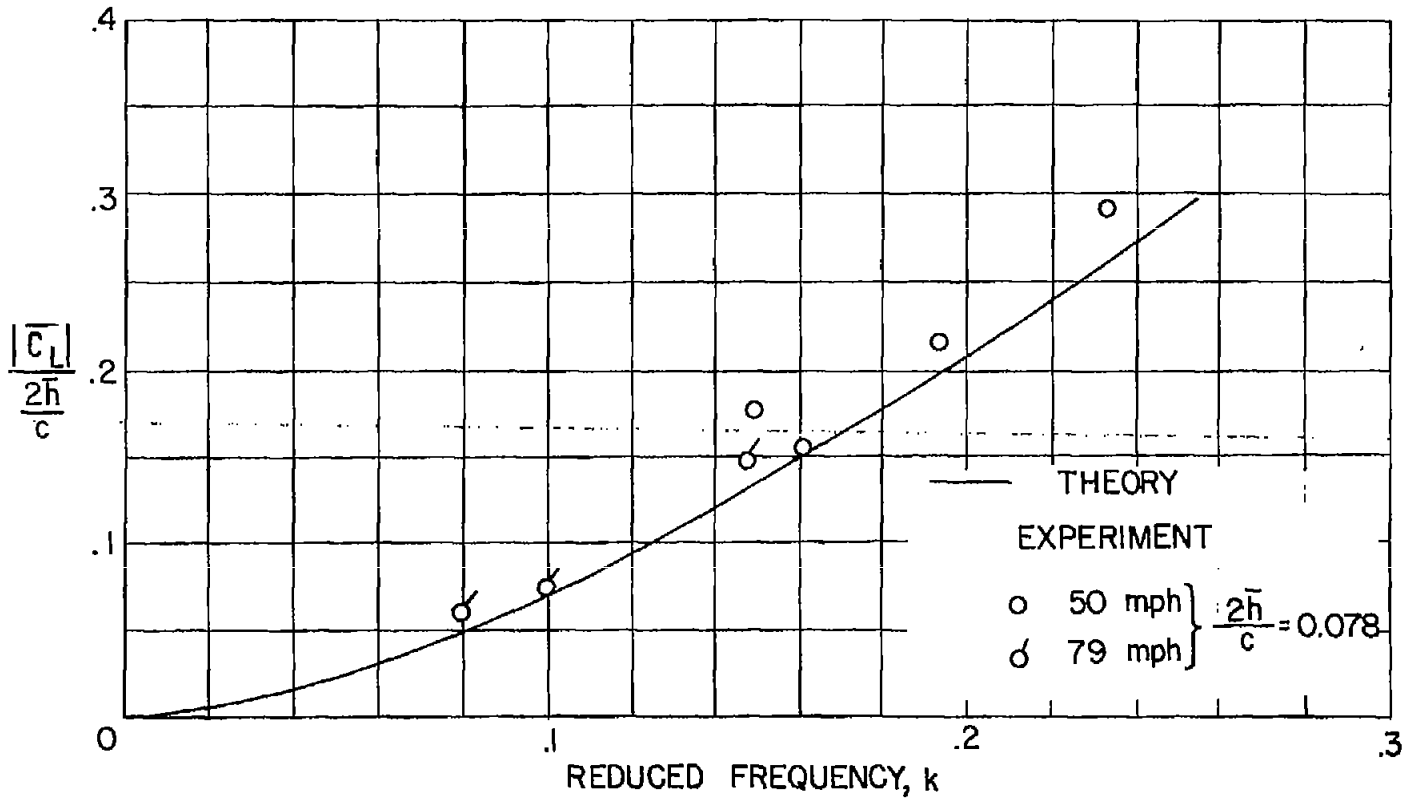

Figure 21.- Measurement of sinusoidal lift.

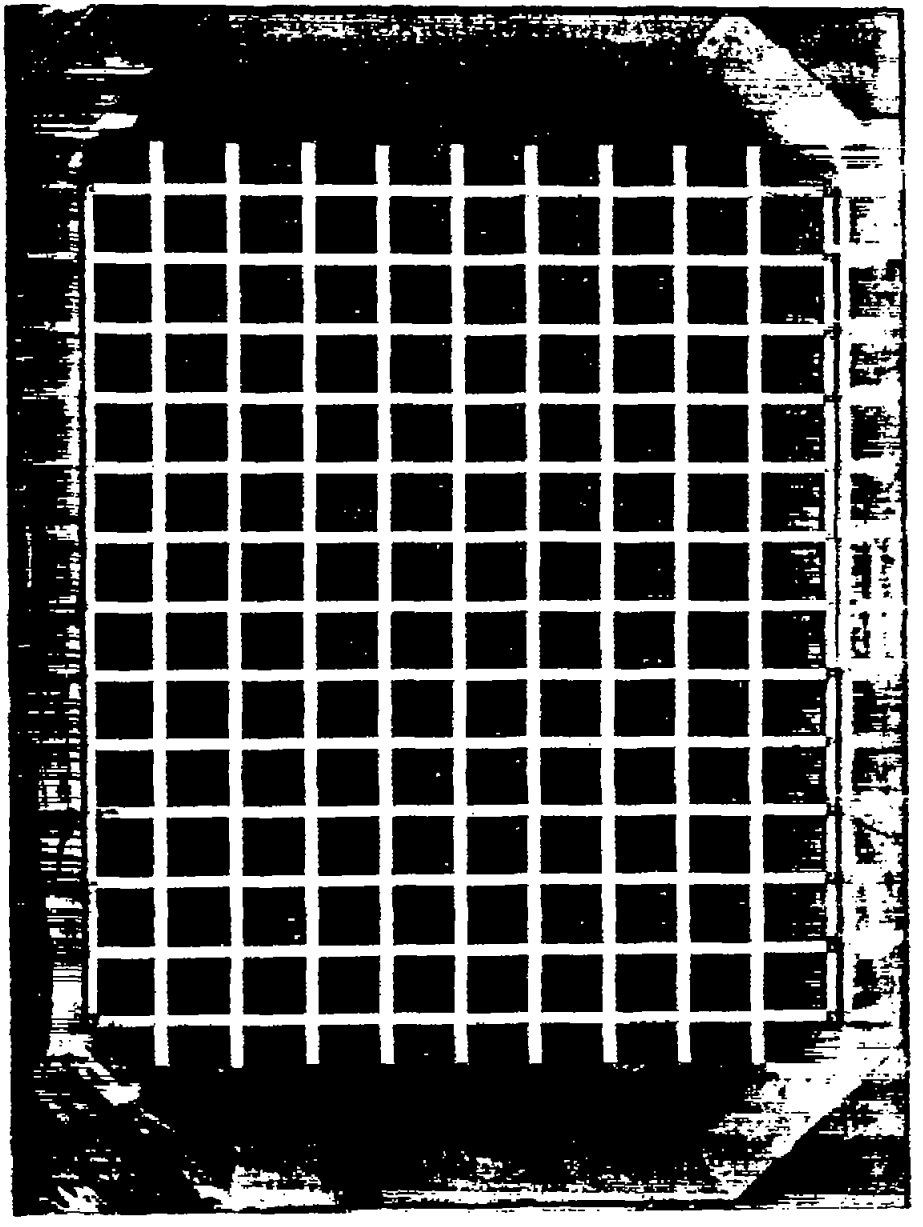

L-95803

Figure 22.- Turbulence-generator grid.

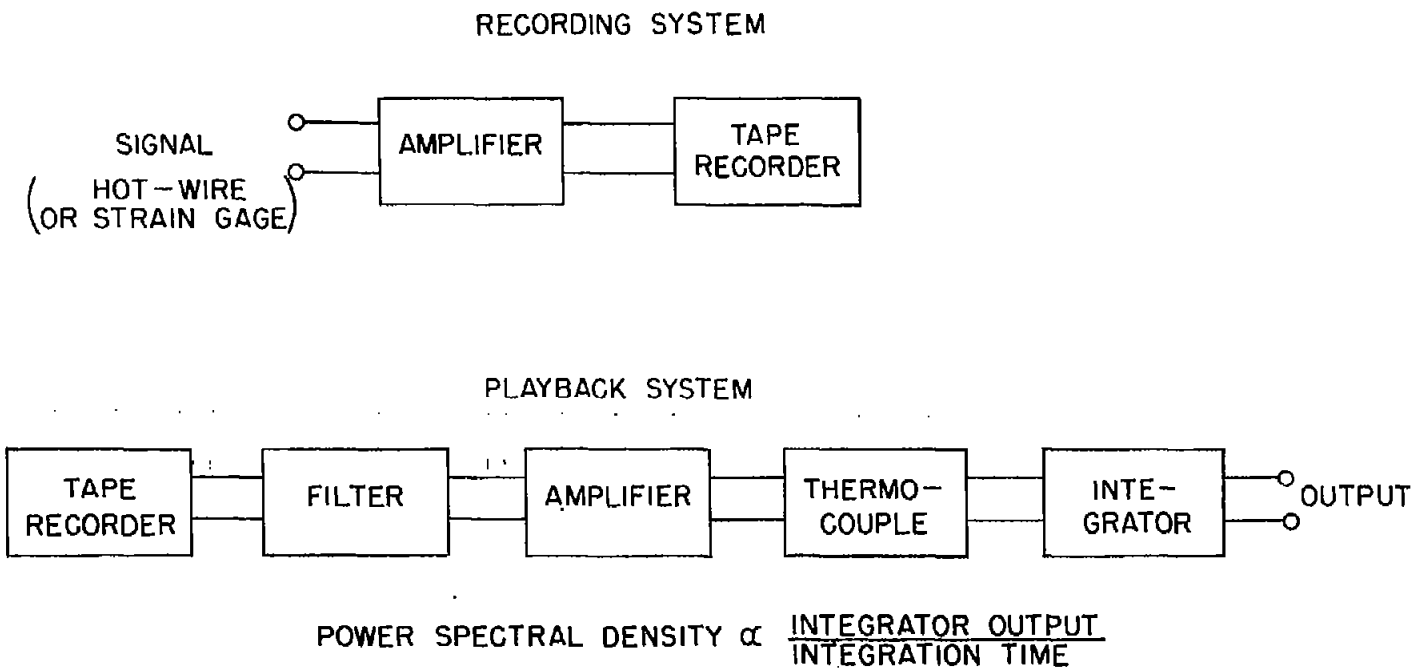

Figure 23.- System diagram for power-spectrum measurements.

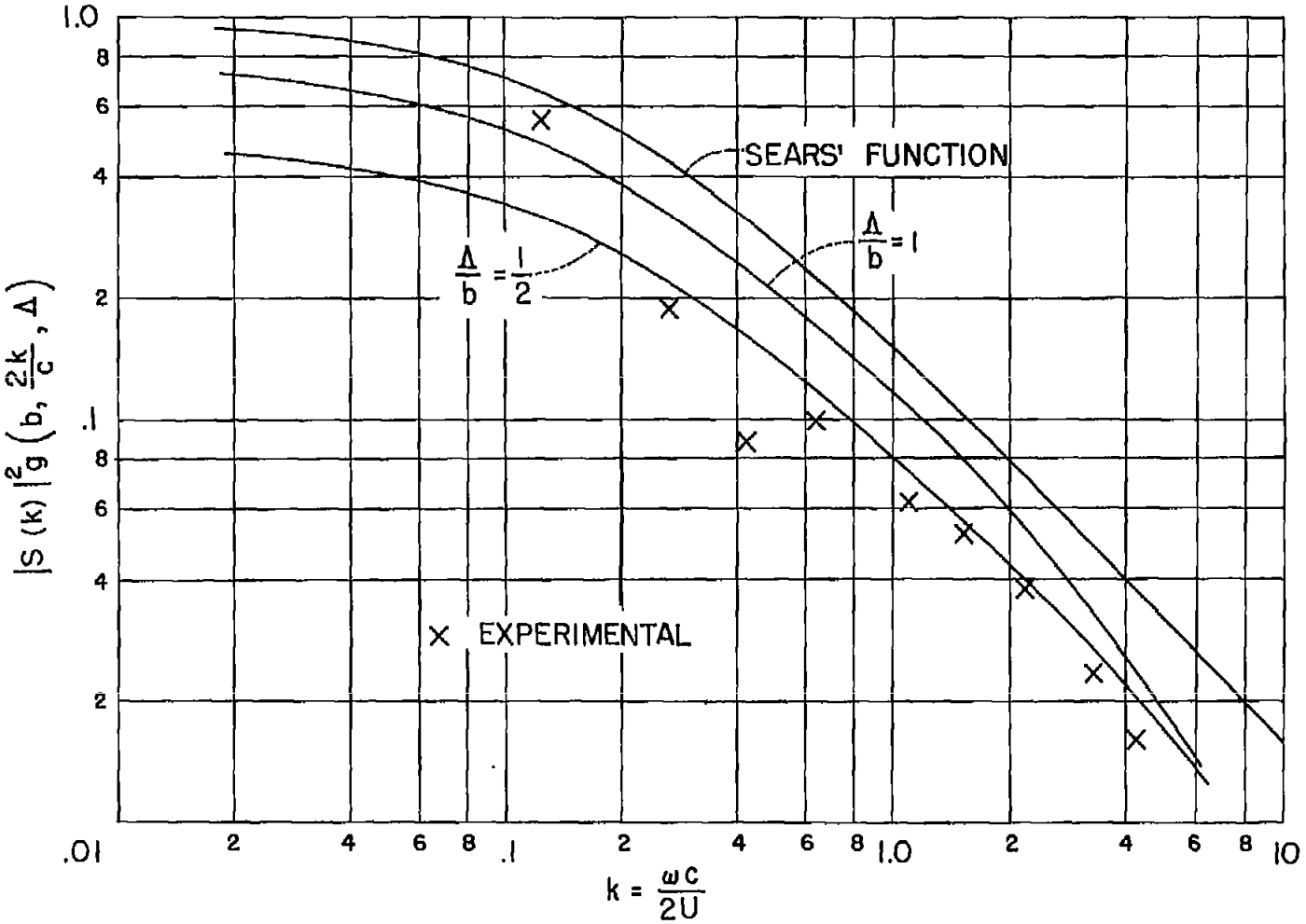

Figure 24.- Comparison of experimental results and theoretical estimate of complete transfer function. b/c = 1/3.

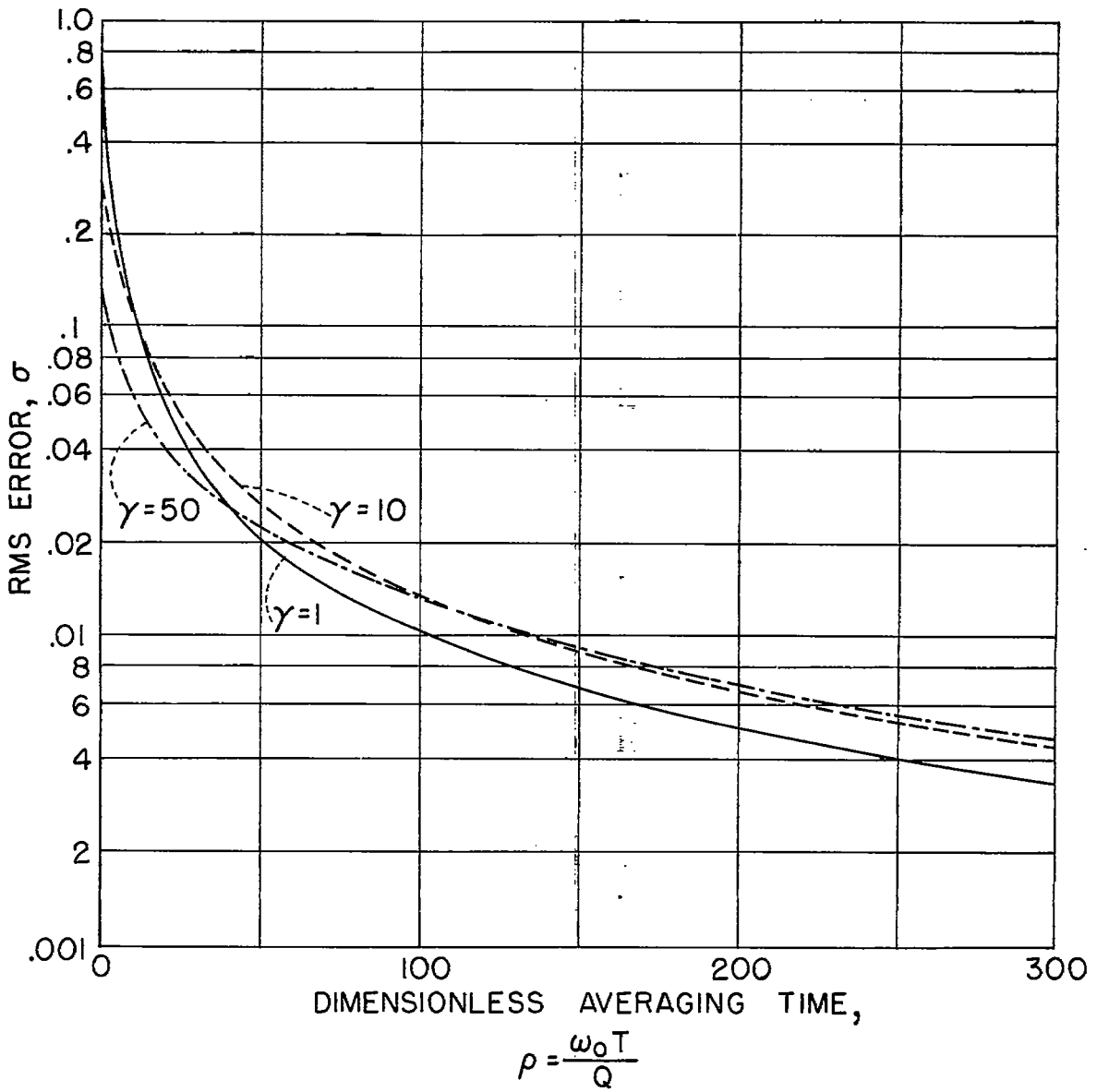

Figure 25.- Statistical root-mean-square error of power-spectrum measurement with filter and time lag. $\gamma = \frac{\omega_o T_c}{Q}$.

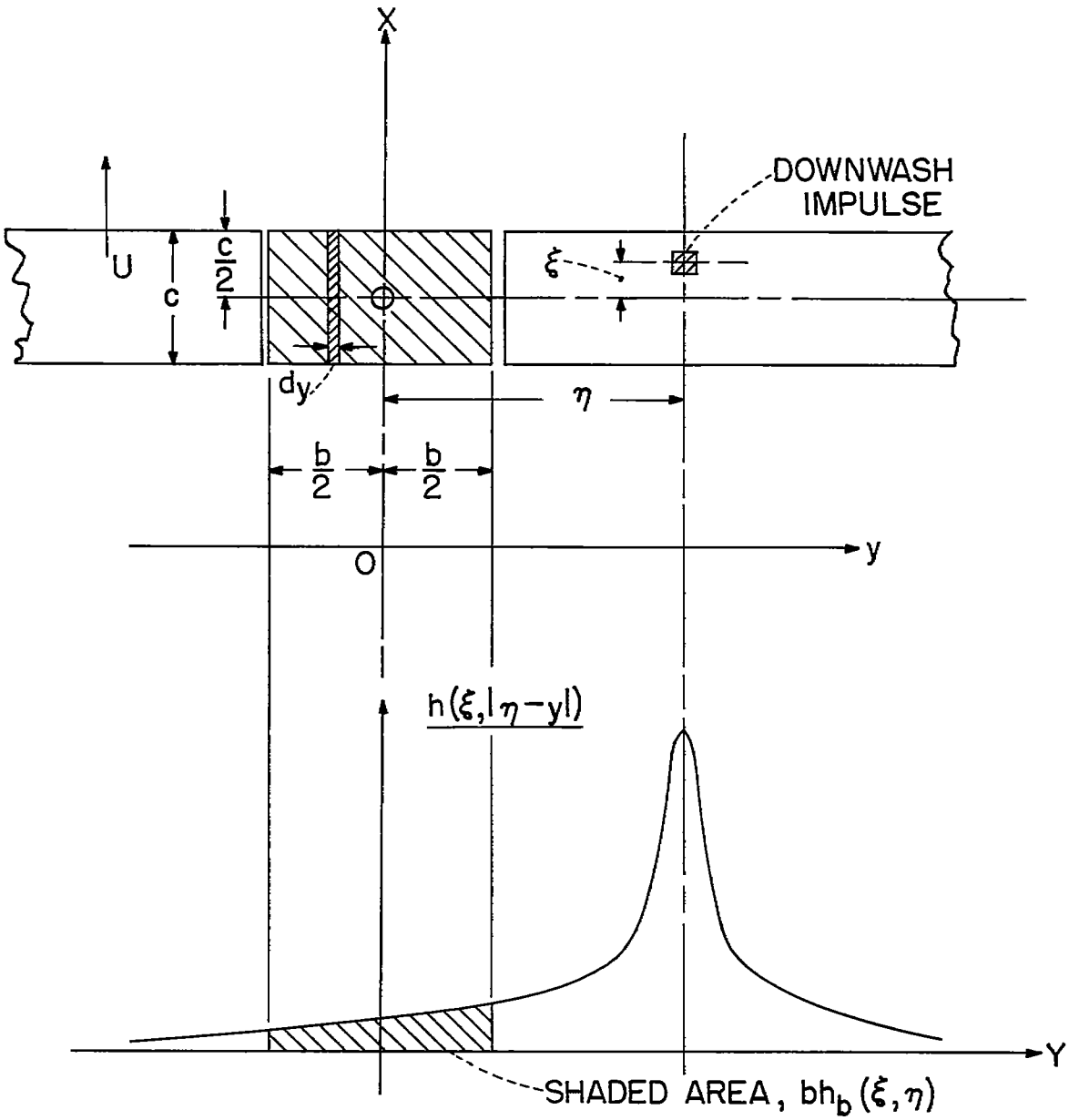

Figure 26.- Coordinate systems and sketch of lift influence function. xy system stationary; ξ η system follows wing moving with velocity U in x-direction.

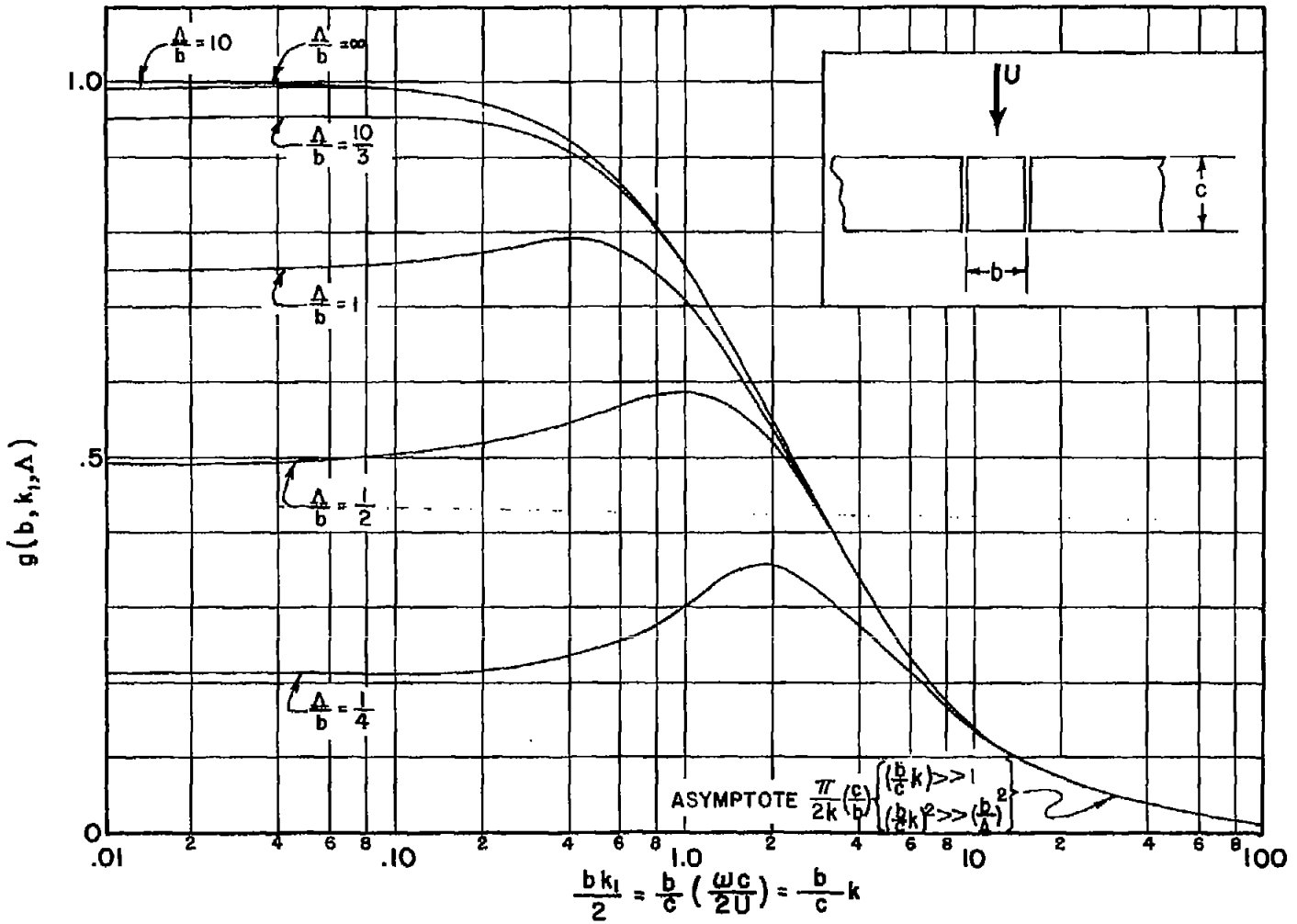

Figure 27.- Finite-span correction.

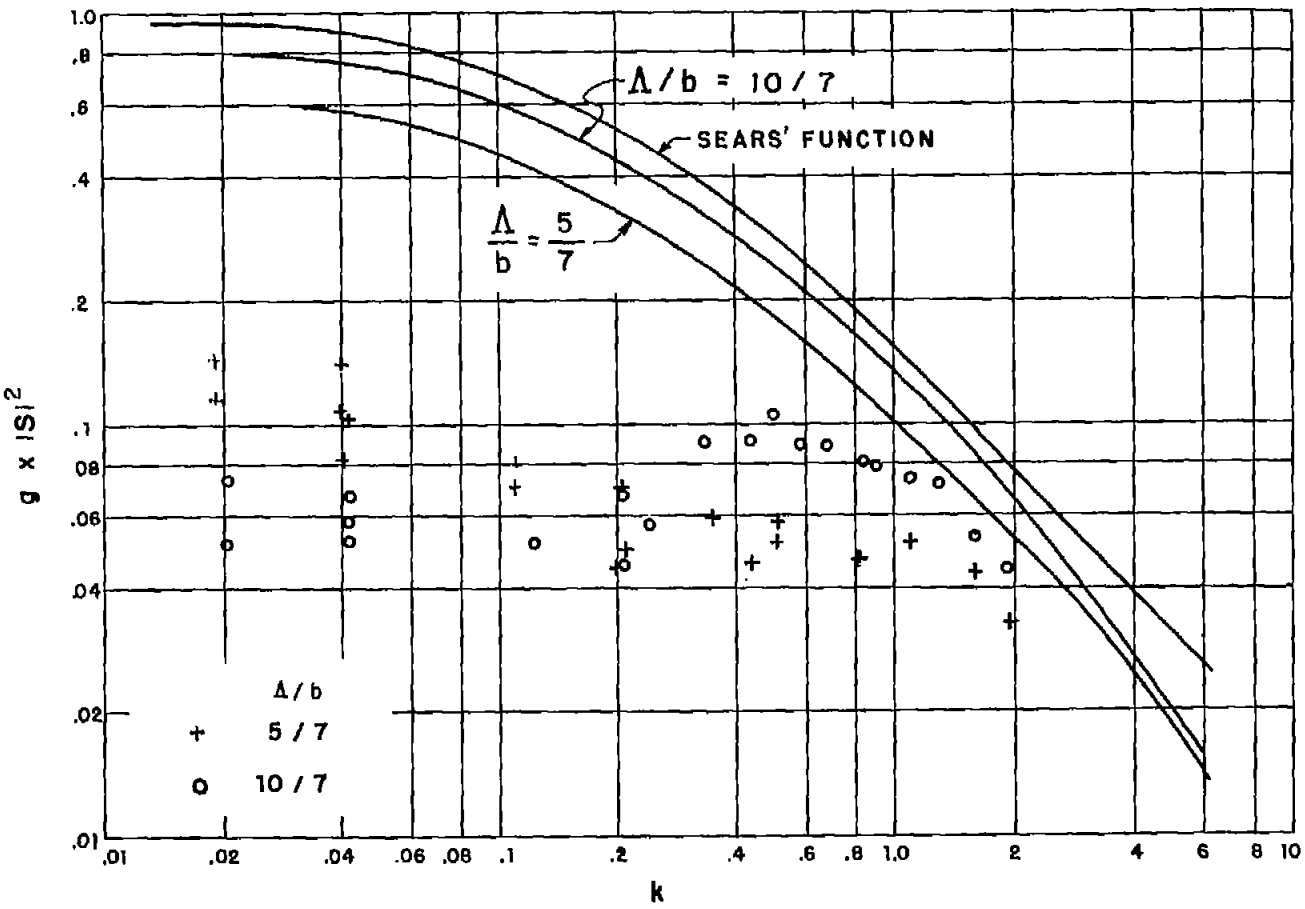

(a) With no end plates.

Figure 28.- Comparison of results of reference 13 to theoretical estimate (b/c) = 0.28).

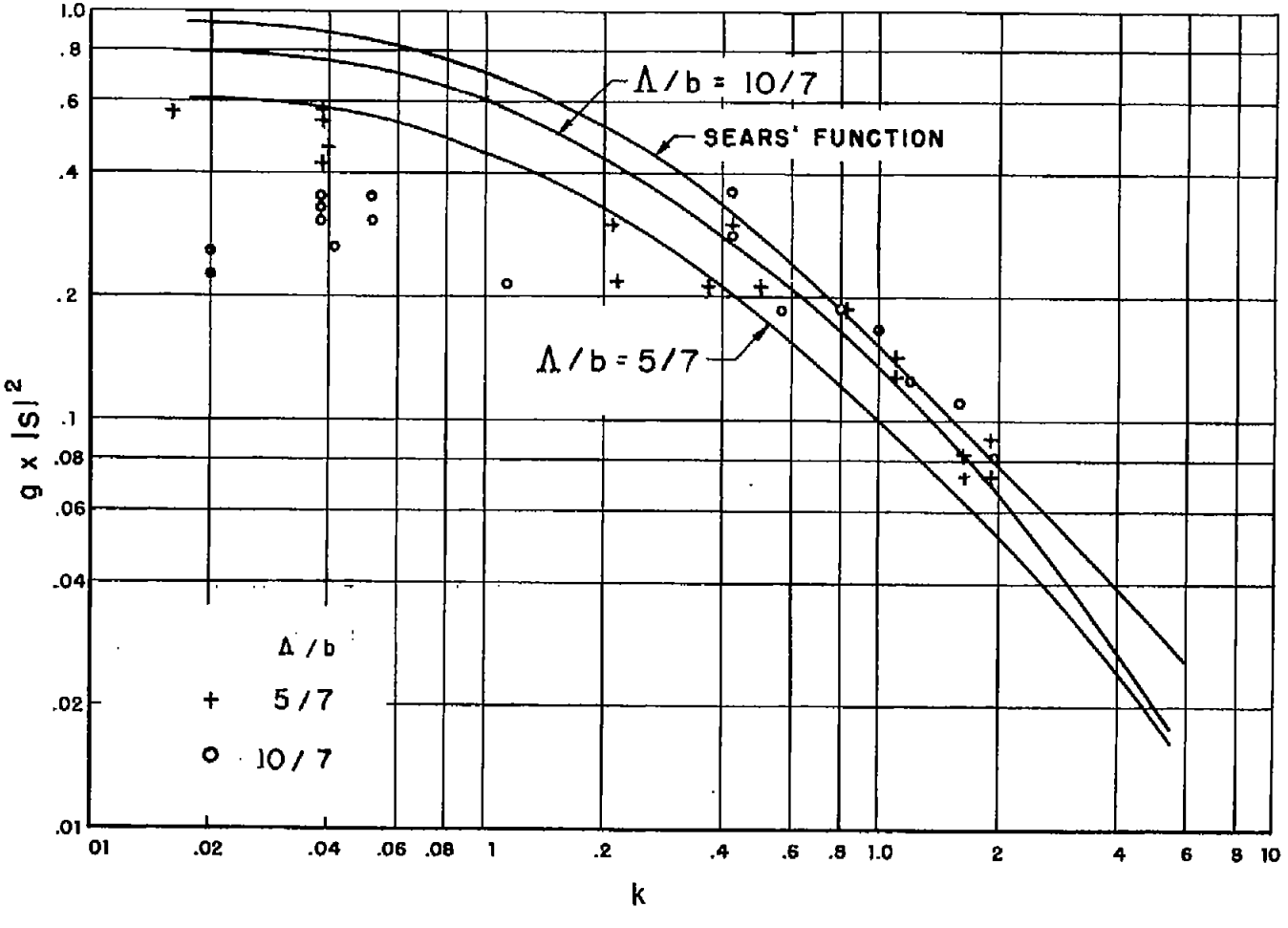

(b) With end plates.

Figure 28.- Concluded.